FINAL REPORT - FLIGHT PHASE

Contract NASw-1388

Rocket Study of the X-Ray Background

31 December 1971

Lockheed

MISSILES & SPACE COMPANY

A GROUP DIVISION OF LOCKHEED AIRCRAFT CORPORATION

SUNNYVALE, CALIFORNIA

FINAL REPORT - FLIGHT PHASE

Contract NASw-1388

Rocket Study of the X-Ray Background

31 December 1971

Philip C. Fisher
Richard C. Catura
Paul Kirkpatrick
Arthur J. Meyerott*
Douglas T. Roethig

Lockheed Palo Alto Research Laboratories
3251 Hanover Street
Palo Alto, California 94304

* Deceased 20 November 1971

I. INTRODUCTION

The activities described in this report were initially directed toward observation and interpretation of the spectra of 0.2-3 keV photons from discrete sources and the diffuse background. It was assumed that the high density of galactic matter at low galactic latitude would lead to measurable absorption effects for the less energetic photons. Although no relevant measurements had been made when the investigation was proposed in June 1965, by 1968 absorption effects in the spectra of discrete sources were becoming fairly well documented through the efforts of other experimental groups. Partly because of this, the investigation was redirected to include the location of x-ray sources as well as information on their spectra. Furthermore, absorption effects of extragalactic matter were sought.

This report briefly discusses the overall effort, and then presents in some detail the characteristics of the x-ray detection system that was to be the primary source of x-ray data. The initial version of this system was described in the January 1966 final report to Contract NASw-909, and by Fisher and Meyerott (1966). The present report concludes with a preliminary assessment of the results from the successful use of the detection system during a June 1971 rocket flight.

II. THE EXPERIMENTS

The basic procedure for making observations was to slowly scan the fields of view of rocket-borne detectors across selected swaths of sky. The Attitude Control System, ACS, developed at NASA's Goddard Space Flight Center, was used to position the rocket properly at the start of each scan, and then to carry out the prescribed scan maneuver. The principal x-ray detection system, designed for 0.2-3 keV x-rays, employed x-ray optics and thin-window gas-flow proportional counters. The x-ray optics consisted of a nested array of mirrors that focussed

an incident plane wave of x-rays to a line shaped image. The focussed x-rays were detected by a proportional counter. This system was supplemented by a Be-window gas-proportional counter for 2-20 keV x-rays. The energy was measured for each x-ray detected. Optical aspect information was to be obtained with the aid of star trackers and a camera. All instrumentation viewed the sky out the forward end of the rocket, after the nose cone had been ejected. Two complete rocket payloads were fabricated, the first for an Aerobee 150, and the second for an Aerobee 350.

The first payload was flown on Aerobee 4.187 on 25 August 1967. To minimize errors in roll, an ACS with a roll-stabilized platform was employed. The observing program was based on three slow scan maneuvers. The first two slow scans were 15° long and normal to the galactic equator at longitudes of 20° and 0°. The third maneuver was to scan the detectors over the x-ray source Sco X-1. Three difficulties were encountered in carrying out this effort.

The first difficulty was that the mirrors of the x-ray optics were not sufficiently rigid and departed appreciably from the desired parabolic curvatures. Radiation from a distant on-axis point source could not be brought to a sharp focus. Image blurring was such that a pair of sources separated by as much as 20 arc minutes could not be resolved. Although the inherent focussing capability of the x-ray optics was not realized, this was not a serious failure because the first rocket flight emphasized measurement of x-ray spectra.

The other two difficulties with the Aerobee 4.187 experiment were serious. First, the programmed slow scans did not traverse the desired portions of sky because of a large error incurred in an earlier roll maneuver. The three maneuvers had been carefully arranged so that both discrete x-ray sources and visibly-bright stars could be observed. Because these scans were displaced appreciably, known low-latitude x-ray sources were not observed and star-tracker

data were inadequate to provide vehicle aspect. Failure to locate and recover the payload caused loss of the aspect information which would have been provided by the camera film. Consequently, no useful x-ray data were obtained from the flight of Aerobee 4.187, and no payload was available for the second flight required by the contract.

Fabrication of a second payload, for Aerobee 17.08, was begun in the fall of 1968. To obtain longer source observing times for increased sensitivity, shorter scan maneuvers and slower scan rates were required than those available on Aerobee 4.187. These requirements were met by a STRAP III attitude control system and rate-integrating gyros. The observing program for Aerobee 17.08 consisted of .03 deg sec^{-1} scans over NGC 4151, 3C273, and a portion of the Virgo Cluster including M 87 and M 84. The flight concluded with a scan over Sco X-1 at a rate of 0.2 deg sec^{-1}. The three difficulties encountered on Aerobee 4.187 were all surmounted with the Aerobee 17.08 payload. The instrumentation on this payload performed very well during flight. The remainder of this report is concerned with a description of the primary x-ray detection system on Aerobee 17.08, and some of the flight results that were obtained.

III. X-RAY-OPTICAL DETECTION SYSTEM

A. Optical Design

The success of the Aerobee 17.08 experiment required an ability to observe soft x-rays and accurately locate the source of their emission. An optimum detection system should have large effective aperture, good angular resolution, a relatively small detector (in order to help minimize particle-related background effects) and the ability to reject non-x-ray pulses. The optical portion of these requirements was met by the system shown schematically in Figure 1. The apparatus is not a true telescope as it provides a line image, rather than a point image, of a distant point source.

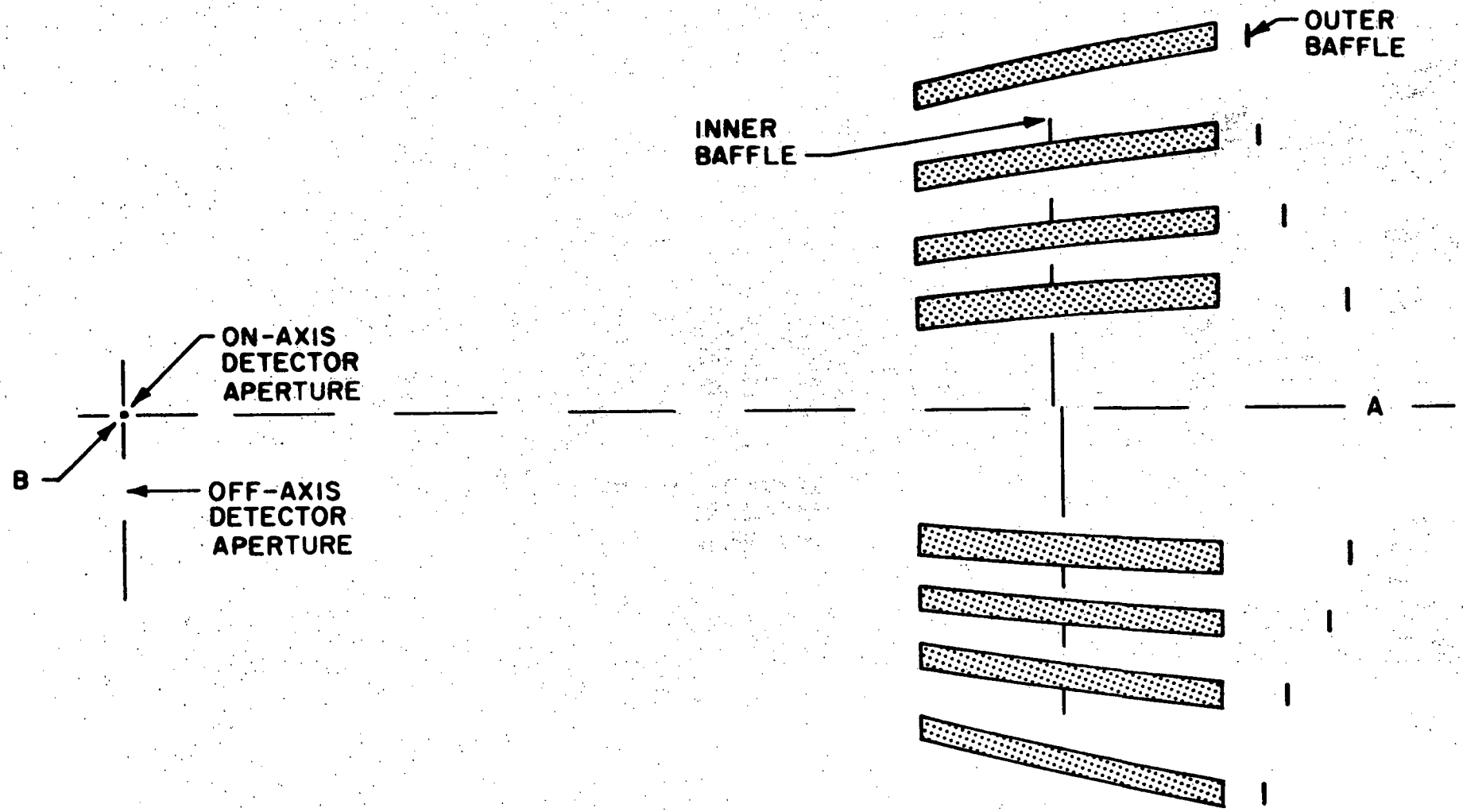

Figure 1 Schematic view of major elements of the x-ray optical system. The stippled areas represent the mirrors whose reflecting surfaces have parabolic cross section. To provide greater clarity, the horizontal scale has been reduced by a factor of ten relative to the vertical scale.

The vertical scale in the cross sectional view given by Figure 1 has been expanded tenfold relative to the horizontal scale in order to more clearly indicate the basic components of the system. The stippled bars represent a side view of the eight rectangular mirrors which have been formed into segments of parabolic cylindrical surfaces possessing a common focal line B and a common axial plane AB (both B and AB are shown in cross section). The desired redundancy of detection was obtained by use of two separate proportional counters. The dimension of the detector entrance windows in a direction normal to the plane of Figure 1 is the same as the width of the mirrors in that direction. The mirrors have been stacked as closely together as possible without having any mirror obstruct the passage of rays bound for either detector window from adjacent mirrors (either before or after reflection).

One of the detector windows lies on the axis of the reflectors and another wider window is approximately 26 arc minutes off-axis. When projected back through the mirrors onto the sky, these windows have fields of view which are 6 arc minutes wide for the on-axis detector and 20 arc minutes for the off-axis detector. The angular response in this direction is nearly rectangular, and the widths given are the approximate full widths. The angular response of these windows in the other dimension is triangular in shape with a full width of 18°. Figure 2 shows the detection system constructed for Aerobee 17.08.

For perfect focussing the parabolas should have been of the form $y^2 = Q(x + Q/4)$ with the respective values of Q listed below. The order in this list is that of the mirrors shown in Figure 1, running from top to bottom.

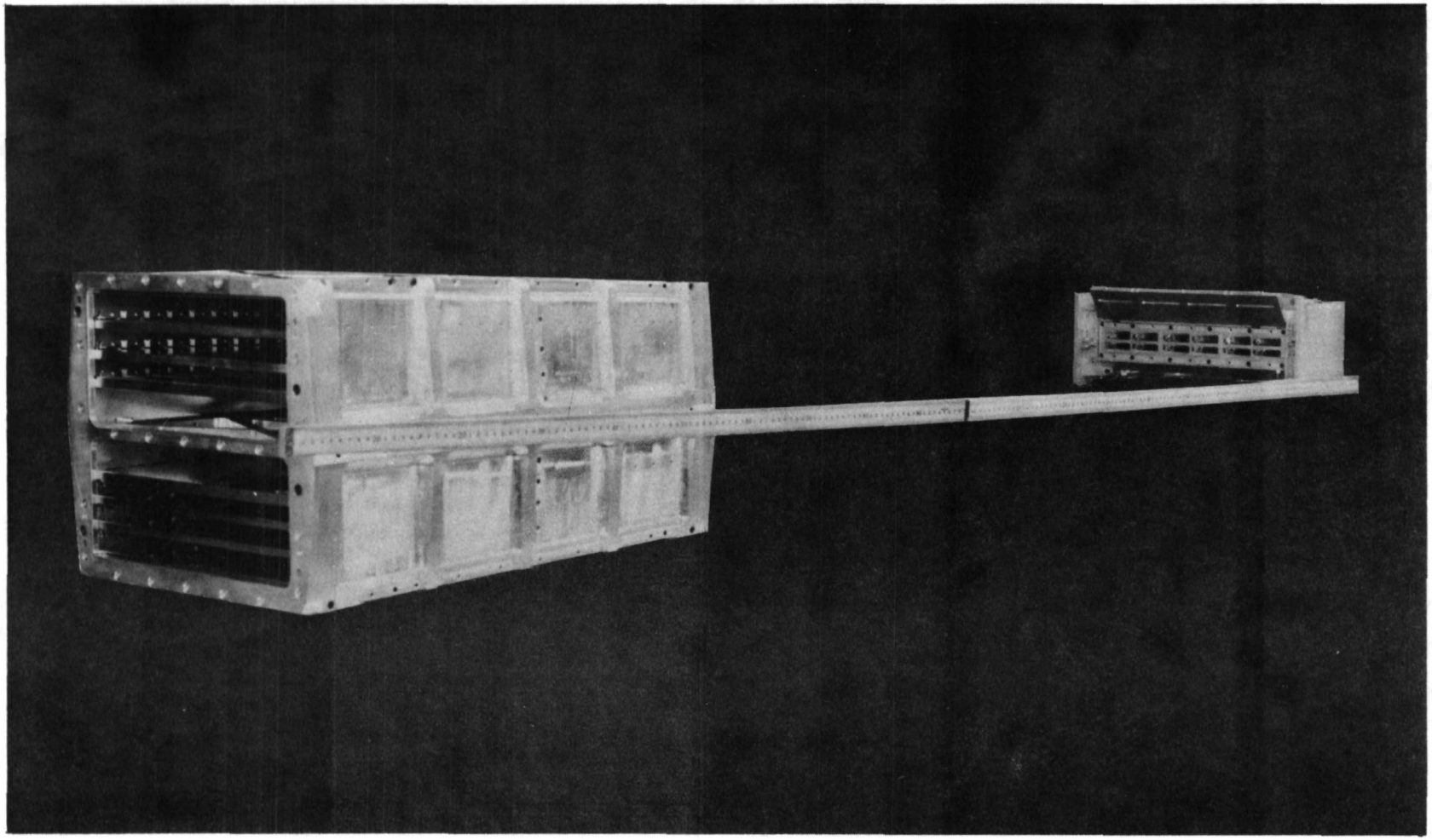

Figure 2. Components of a soft x-ray detection system. A nested array of eight parabolic reflectors is at the left, while two independent x-ray detectors appear at the right of the figure. Not shown in the figure is the set of entrance baffles used to restrict the directions from which x-rays can be accepted.

$Q_1 = 0.306479$ $\quad$ $Q_{-4} = 0.043561$

$Q_2 = 0.161481$ $\quad$ $Q_{-3} = 0.099571$

$Q_3 = 0.074435$ $\quad$ $Q_{-2} = 0.180566$

$Q_4 = 0.022287$ $\quad$ $Q_{-1} = 0.306479$

The asymmetry of these parabolas was dictated by the asymmetric location of the outer edges of the two detector entrance windows.

The baffles shown in Figure 1 were placed so that they did not obstruct rays which would enter a detector window via reflection from the mirrors. All other rays were intercepted either by the baffles or non-reflecting portions of the mirrors. The adopted location of the baffles was not unique, but that which required only a modest forward extension of the baffles into the space at the entrance end of the reflector array. This extension was arbitrarily restricted to some ten percent of the distance between the focal plane and the leading edge of the mirrors.

Figure 3 shows the geometry used for determining the equations of the baffle positions and the useful (reflected) and leakage (unreflected) beam dimensions. The outer edges of the detector entrance windows and the size, position, and shape of the mirrors in the array determine the position and dimensions of the baffles.

The position of the inner baffle for each mirror was evaluated first. By writing the equations of the lines represented by ray A and ray B and finding the intersection of these two lines, one can determine the position of the edge of the inner baffle for each mirror:

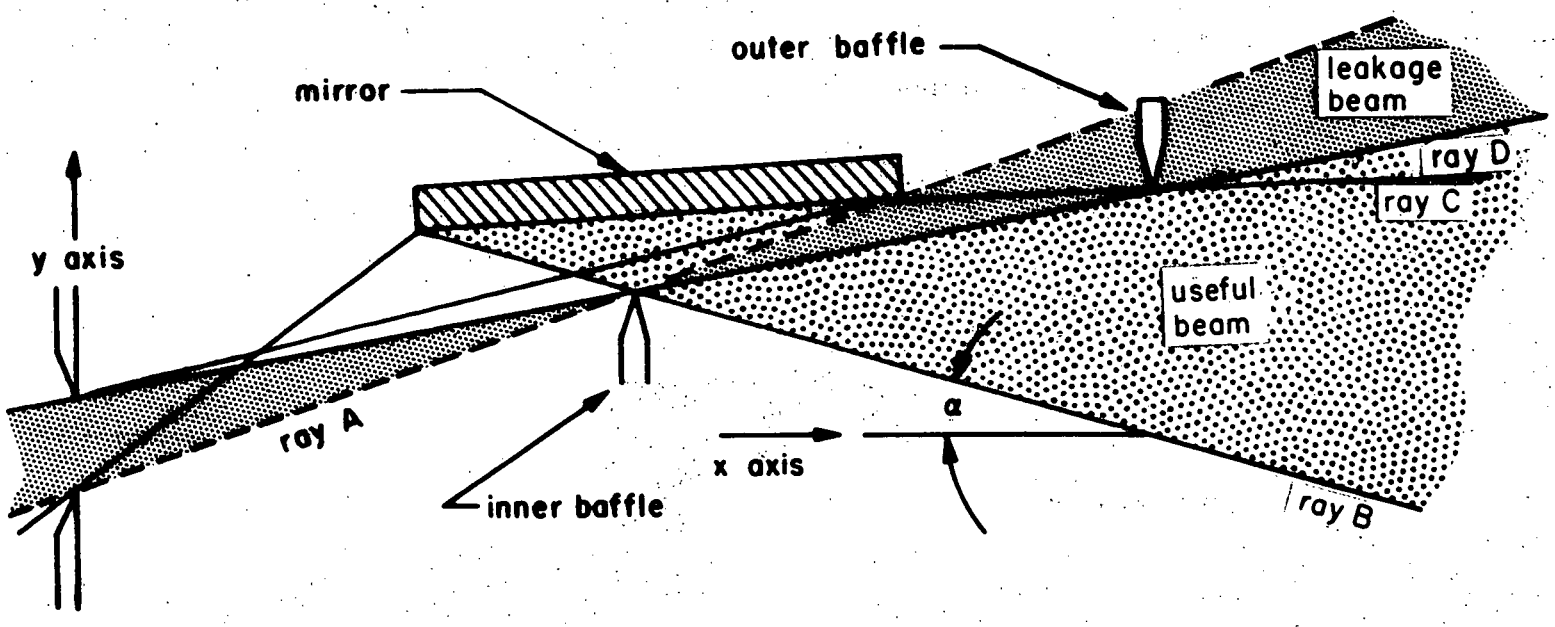

Figure 3 Interrelation of mirror and baffles required to prevent unreflected x-rays from reaching the detectors.

$$x_i = \frac{kL \tan \alpha_D + G - y_D}{\tan \alpha_D + H/L - y_D/L}$$

$$y_i = \left(\frac{H - y_D}{L} \right) x_i + y_D$$

Similarly, the position of the edge of an outside baffle for a given mirror is determined by the intersection of ray C and ray D, so that:

$$x_o = \frac{L \tan \alpha_U + y_U - H}{\tan \alpha_U + y_U/x_i - y_i/x_i}$$

$$y_o = \tan \alpha_U (x_i - L) + H$$

where:

a) the coordinate system origin is in the detector entrance plane,

b) y_U and y_D are the y coordinates of the upper and lower limits of a detector aperture,

c) (kL, G) and (L, H) are the coordinates of the ends of the reflecting faces of the mirrors; where (kL, G) refer to the end nearest the detector,

d) α_U and α_D are the angles the incident radiation must make with respect to the x-axis in order to be reflected to the upper and lower limits respectively of the detector aperture.

In actual practice, the baffles were constructed from ground steel rods, whose curved surfaces contained the baffle extremes defined by y_i and y_o above. Appendix A contains the code used to calculate the precise values of the coordinates for the limiting edges of the baffles.

B. Fabrication of Mirrors

Each mirror was produced as an optical flat. The basic component was a 12 inch x 20 inch sheet of instrument-grade, HP 20, hot-pressed beryllium. This substrate was chosen because of its high strength-to-weight ratio. The non-reflecting side of each sheet was machined to

form a series of stiffening ribs which were parallel to the 12 inch dimension of the mirror. Stresses in the beryllium created during the machining process were relieved by temperature cycling the blanks while they were pressed between a pair of heavy steel plates. Acceptable annealed blanks were required to be flat to within .003 inches over their entire surface. Each of the coating materials which was deposited on the Be substrates was approximately 90 percent nickel and 10 percent phosphorous. Six of the mirrors were coated with .005 inches of Kanigen, and two were coated with .010 inches of Nye Kote. These trade names refer to the process by which this material was deposited. After the nickel coating, a pair of blanks were set in wax on a supporting table and the mirror surface created by conventional optical grinding and polishing techniques.

The curvatures required of the mirrors were attained by pressing each reflector against a pair of parabolic aluminum templates which extended along the edges of its 20 inch dimension. Force was applied to each rectangular mirror along these templates by the manner shown in Figure 4. Forty compression springs pressed the reflecting face of the mirror against forty precisely machined pads on each template, the pads lie on chords of the required parabola to within about 0.0001 inch. Forces applied by these springs ranged from 13 to 18 pounds with the greater force at the ends of each mirror.

C. Parabolic Nature of Individual Mirrors

We were quite aware that this method of fabricating the mirrors would not yield reflection optics of telescope precision. However, it seemed clear that this approach would fulfill requirements of the proposed experiment. We foresaw in general the departures from perfect parabolic cylindricity, realizing that even if the supported edges could have been brought to perfect parabolas, the intermediate areas would have assumed other curvatures subject to the reluctance of all parts of the mirror to comply with the deforming forces.

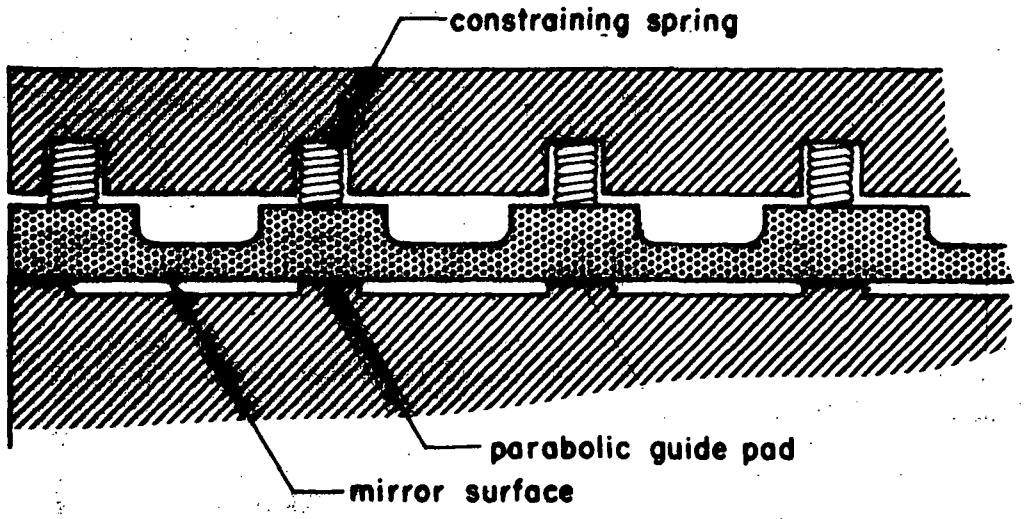

Figure 4 Cross sectional view indicating how a flat mirror was constrained to a parabolic shape.

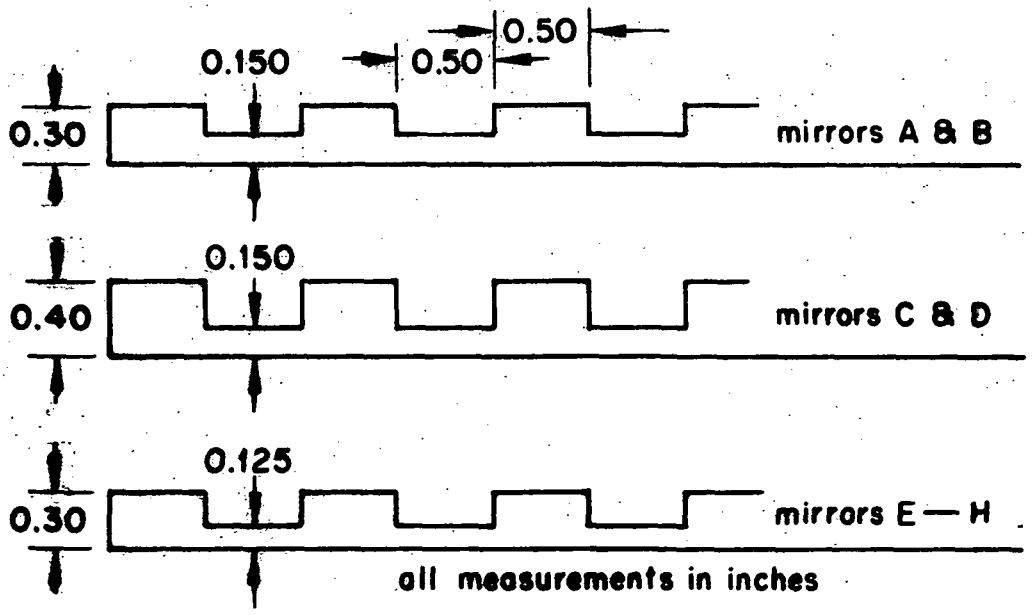

Figure 5 Cross sectional view of the various Be blanks used in fabricating the Aerobee 17.08 mirrors. The dimensions are given in inches.

The flight experiment required that the departures from desired curvature lead to a degradation of angular resolution that was substantially smaller than the 6 arc minute wide entrance to the on-axis detector of Figure 1. As discussed later, the 17.08 reflector array satisfied this requirement very well.

Aerobee 17.08 mirrors were made with stiffening ribs one-half inch wide, rather than one-quarter inch wide as were the 4.187 mirrors, to provide greater rigidity. Mirrors were fabricated to the three different cross sections shown in Figure 5. These configurations were chosen to determine the sensitivity of a mirror's figure to simple variations in its construction.

Figure 6 indicates the response obtained from mirror B when constrained by parabolic guides having $Q_2 = 0.16$, and illuminated by an on-axis beam of 1.5 keV x-rays. The center curve is a profile of the angular spread of the incident x-ray beam while the outer curve gives the profile of the beam reflected from this mirror when the portion of mirror midway between the parabolic templates is illuminated. The behavior of the entire mirror was determined by reflecting x-rays from surface elements distributed successively along the length of the mirror and measuring the deviation of the reflected beams. The maximum amount of divergence comes from portions of reflecting surface near the entrance and exit edges of the mirror. If the entire mirror were uniformly illuminated, the divergence is such that about four-fifths of the reflected radiation has an angular spread of less than two arc minutes and the remaining one-fifth is contained within an angular interval of eight arc minutes.

Most of the measurements of the parabolic figure of the various mirrors were made using a parallel beam of visible light. Since the reflection is specular at both wavelengths, it is valid to use visible light instead of x-rays to investigate the geometrical properties

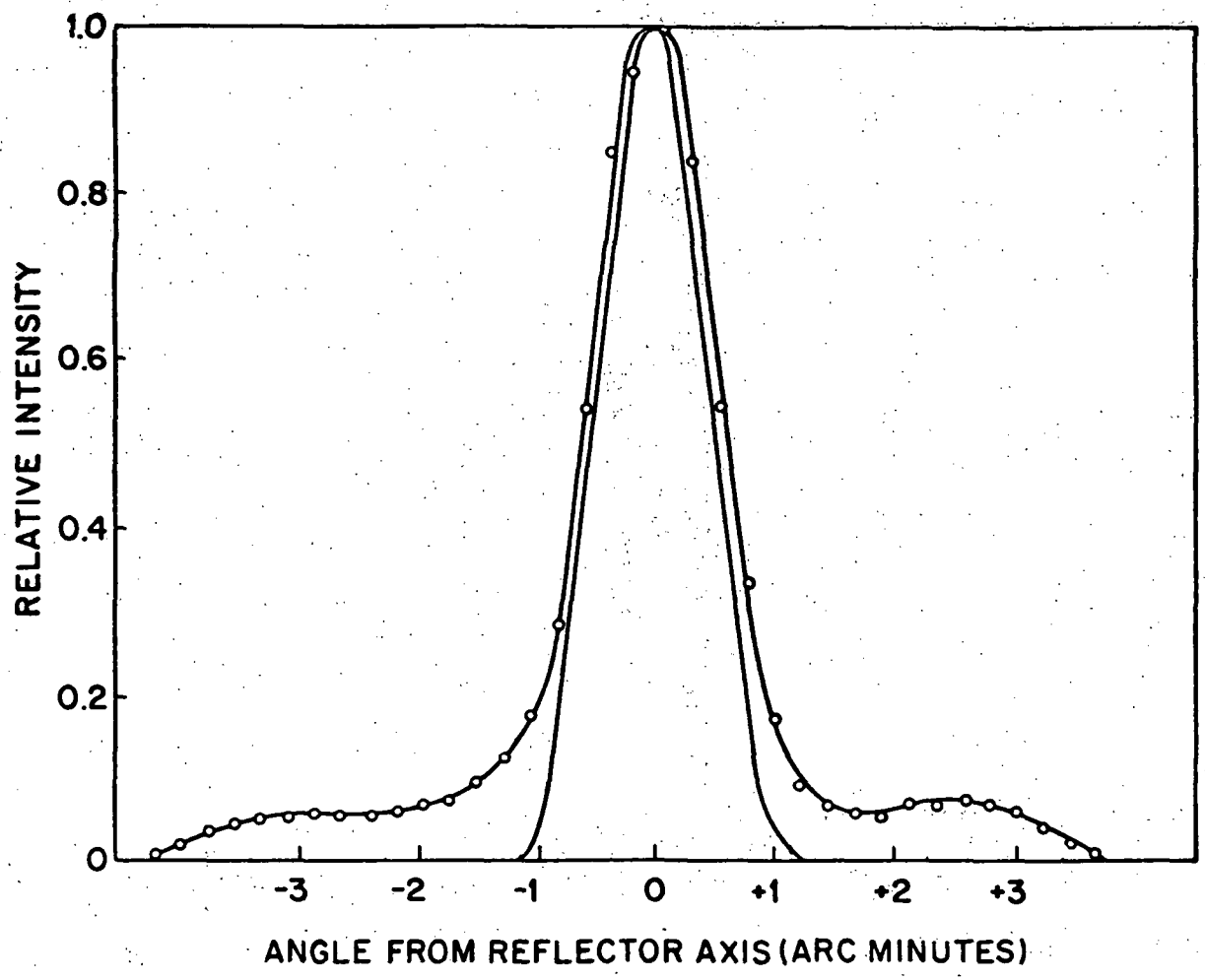

Figure 6 Profile of the incident and reflected 1.5 keV x-ray beams for a typical parabolic mirror. The reflected beam is indicated by the line through the open circles.

of the mirrors. As had been anticipated, a given mirror conforms less well to a parabola as the curvature of the parabola is increased (i.e., as the value of Q is increased). However, so little difference was found when the mirrors of different cross sections were pressed against a given parabolic guide that only a qualitative indication of the performance seems worth giving here. Mirror E of Figure 5, with the least amount of beryllium between the transverse strengthening ribs, and a 5 mil nickel coating, conformed best to the parabolas. Mirror G of Figure 5, with the same cross section of beryllium as mirror E, and a 10 mil nickel coating, was found to conform less well to the parabolas than any other mirror tested. Even so, with mirror E on the most-curved parabolic guides, the total spread of the reflected beam of the on-axis source was no more than some ten minutes of arc, again with approximately 80 percent of the total within a few minutes of arc. Mirrors A-D were found to be of intermediate stiffness and not significantly different from each other.

The focal properties of this type of parabolic reflector are such that the width of the line-shaped image of a point source increases as the off-axis angular distance of the source increases. As a result, this type of optical system gives precise position information for a relatively narrow field of view. The blurring of a source image is directly related to the fraction of the overall length of the system occupied by the mirrors, and can be decreased by use of shorter mirrors.

The angular resolution of the assembled array of mirrors, as measured with visible light, is shown in Figure 7. The full width at halfmaximum of the reflected beam from all 8 mirrors is 0.9 arc minutes. The response given in the figure is appropriate for focusing of low energy x-rays, since all the mirrors reflect such x-rays with equal efficiency.

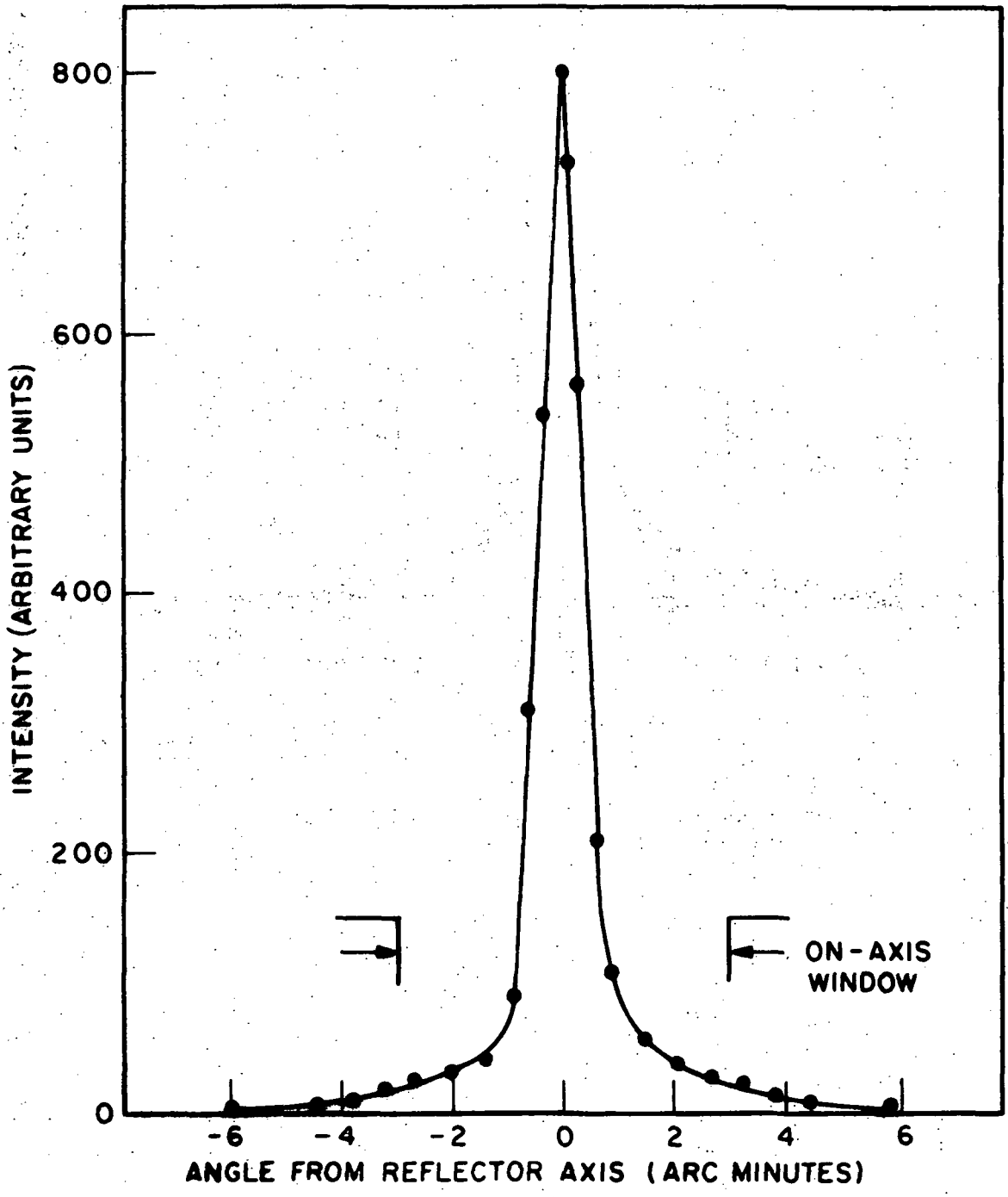

Figure 7 Image profile of an on-axis beam of visible light reflected from all eight mirrors of the array. The reflector is illuminated by a band of parallel light 1/2 inch wide which extends across all eight mirrors approximately midway between the parabolic mirror guides. The size of the 6 arc minute wide detector window is indicated by the arrows.

D. Effective Aperture of Mirror Array

To obtain the effective aperture of the optical system, it is necessary to know each mirror's efficiency for reflection as a function of incident angle and x-ray energy. The reflection efficiency of one of each of the four pairs of Aerobee 17.08 mirrors was measured with 1.5 and 4.5 keV x-rays. Average values of the measured efficiency as a function of angle of reflection are given in Figure 8. Although the mirrors were fabricated at different times, and no special storage precautions were taken, the variation of efficiency with angle was found to be independent of time and of the particular mirror surface examined. However, surface irregularities of the flight mirrors were such that a significant portion of the incident radiation was non-specularly reflected. The significance of this non-specular component seems to increase as the x-ray energy increased. It is interesting to note that the non-specular component measured from an optical flat of pyrex was negligible. Also given in Figure 8 is an efficiency for reflection of 0.28 keV x-rays. The decrease in reflection efficiency at small angles for this energy is not understood at this time. Considerable effort was made in repeating the measurements attempting to discover possible systematic errors, but none have yet been found. Since only a small portion of the reflector array has angles of incidence less than 1° for x-rays reflected into the detector windows, this decrease in efficiency at 0.28 keV does not seriously affect the aperture of the system. Calculations described below indicated that this effect decreases the effective area of the system by approximately 5%.

For x-rays between the 1.0 keV L-edge and the 8.3 keV K-edge of nickel, the data of Ershov et al. (1967) were combined with information of Wuerker (1960) to derive an index of refraction for the reflectors as a function of x-ray energy. The linear absorption coefficient of nickel in this energy range was obtained from Veigele et al. (1969). Using this information, and a procedure described by Rieser (1957),

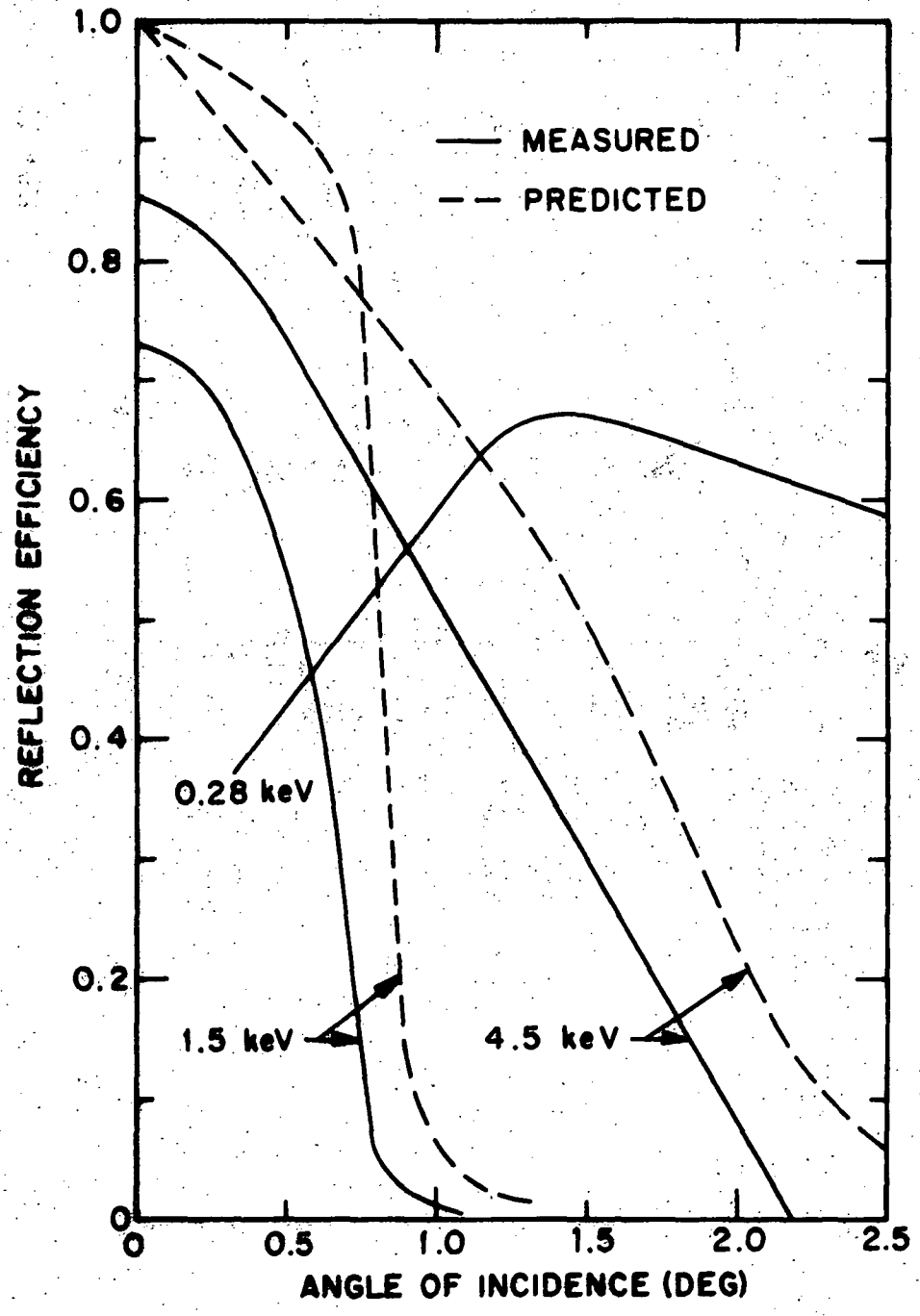

Figure 8 Reflection efficiencies for nickel mirrors. The measured results for 1.5 and 4.5 keV are the average values from four flight mirrors. The 0.28 keV measurements are from a single mirror and remain to be verified. The text describes how the predicted efficiencies were obtained.

the code of Appendix A was used to derive the variation of reflection efficiency with angle of reflection for different x-ray energies. The predicted efficiencies given in Figure 8 were obtained in this manner. The effective aperture of the mirror array for x-rays between the nickel K and L edges can also be calculated with the code of Appendix A. While this code was convenient for comparing the performance of different optical systems for an on-axis source, the code of Appendix B was used to obtain an effective aperture more directly applicable to reduction of flight data. The latter code utilizes either the measured or predicted reflection efficiences of Figure 8 to derive the effective aperture of the optical system as a function of x-ray energy and the off-axis angle of the source. Figure 9 shows one of these response curves for the off-axis detector at an x-ray energy of 1.5 keV. Similar curves were calculated at other energies and integration over the angular coordinate leads to the values of mirror system response given in Figure 10. The variation of this response with energy, above the L absorption edges of nickel, was determined by using the predicted reflection efficiencies of Figure 8. The resulting data were fitted to a polynomial function and normalized to pass through the points calculated from the reflection efficiencies measured from the flight mirrors at 1.5 and 4.5 keV. For x-rays less energetic than the 0.85 keV L-edge of nickel, effective apertures were computed using the data of Ershov et al (1967), and normalized with the 0.28 keV data of Figure 8 from flight mirrors. A linear interpolation was used across the L absorption edges between 0.85 and 1.0 keV. When divided by the rocket scan rate in degrees per second, the ordinate of Figure 10 gives the effective exposure to an x-ray source (not including counter efficiency) in units of cm^2 sec. These data have been used in preliminary analysis of data from the rocket flight described later in this report.

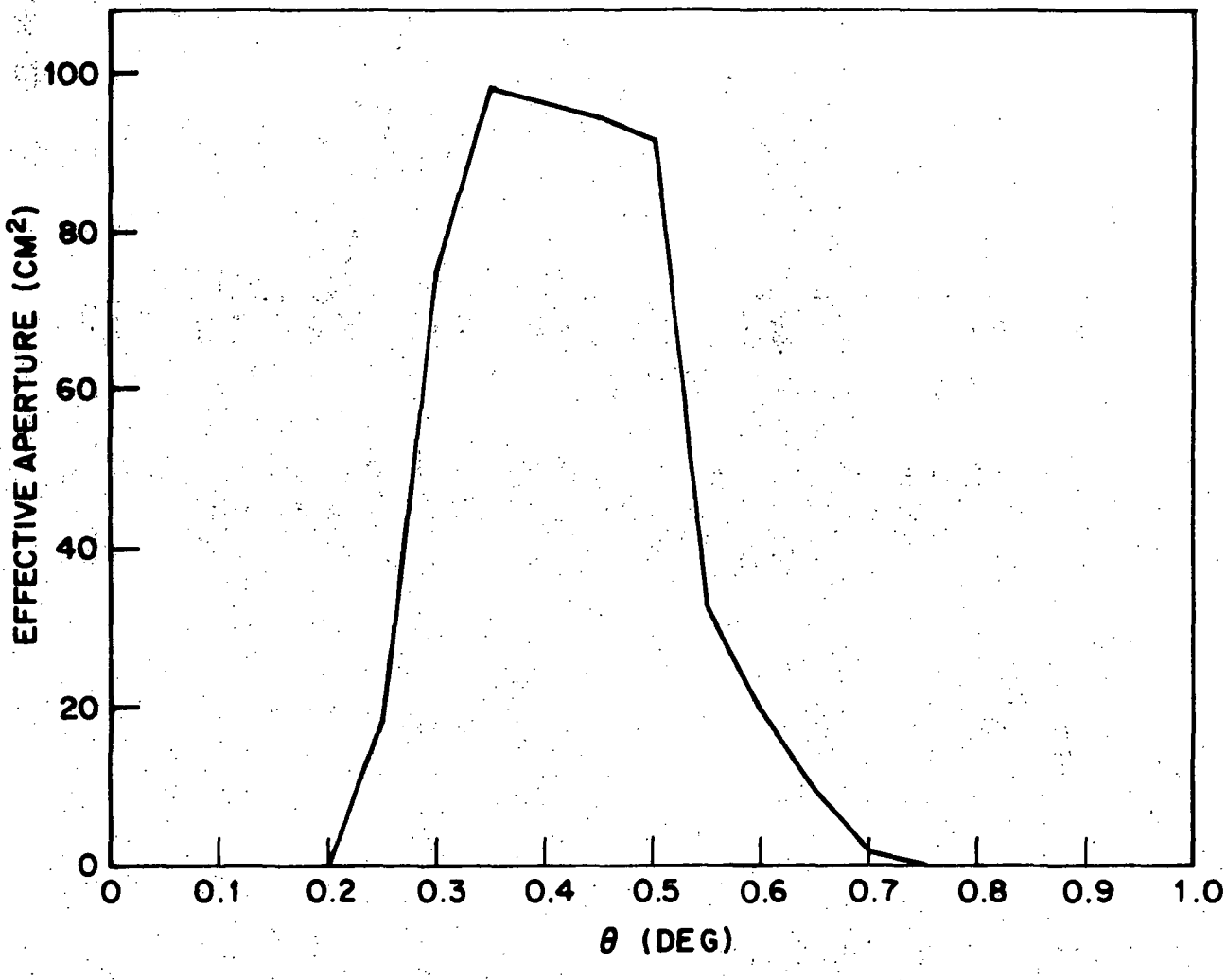

Figure 9 Effective aperture at 1.5 keV for the off-axis detector of Aerobee 17.08 as a function of the angle between an x-ray source and the axis of the reflector array. The predicted efficiency at 1.5 keV of Figure 8 has been used for this calculation.

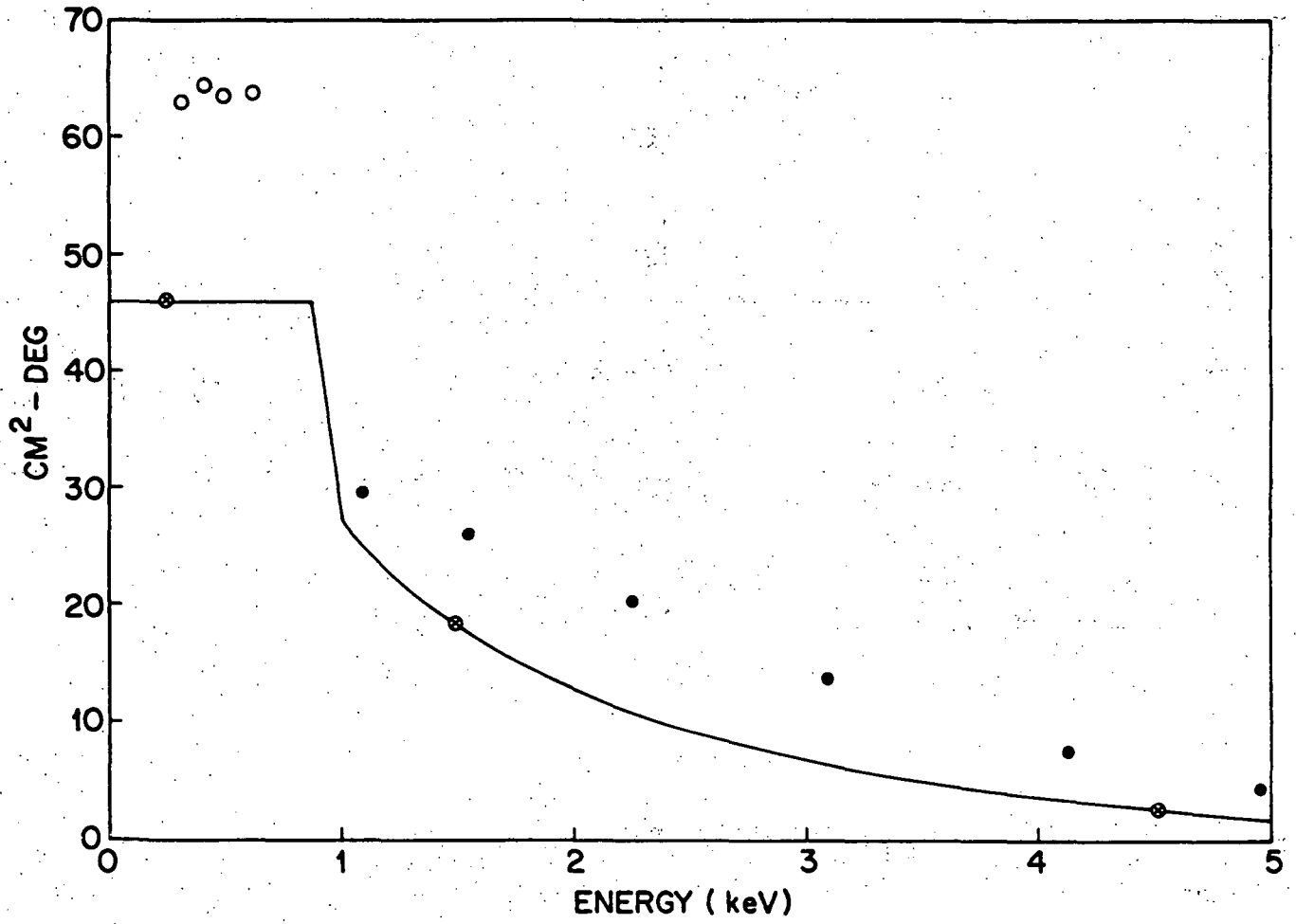

Figure 10 Response of the mirror array as the field of view of the off-axis detector is scanned across an x-ray source. Exposure to the source in units of cm^2 sec as a function of x-ray energy is obtained by dividing the ordinate of this plot by the scan rate in deg sec^{-1}. A detector of unit efficiency was assumed. The points on the graph are the result of using reflection efficiencies from: ⊗ - measurements on the flight mirrors, O - values from the data of Ershov et al.(1967), and ● - calculations described in the text involving the index of refraction and mass absorption coefficient of nickel.

E. X-Ray Detectors

A pair of gas flow proportional counters with thin plastic windows was used to detect x-rays reflected by the mirrors. Figure 11 shows a cross sectional view of the detector system in a plane normal to the line focus of the mirror array. A solid wall divides the two counters which have separate gas supplies. Each x-ray detector is composed of two chambers in tandem separated only by several .002 inch tungsten wires which are at ground potential. Signals from each center wire of the primary detectors are pre-amplified and combined for energies greater than 0.5 keV. Only pulses from the front chambers are analyzed at energies below 0.5 keV. Gas anticoincidence counters are located along two sides of each primary detector. These counters share a common gas supply with the primary detector and are electrically separated by a thin wall of electroformed BeCu mesh. Events which produce ionization in both primary and anticoincidence detectors are eliminated by the anticoincidence circuitry.

The detector windows lie in the focal plane of the mirror system and define the angular acceptance of each counter. The window material is approximately 1 micron of polypropylene coated with 200 A of Al. This material is supported on photo-etched BeCu mesh which is 70% transmitting. An evacuated antichamber was provided in front of each detector so that the same relative pressure could be maintained across the thin plastic window on the ground as in space. In Figure 11 the lid to this antichamber is shown in the open position that is characteristic of the prime data-taking-portion of the rocket flight.

Gas was supplied to the proportional counters by gas flow systems at a pressure of 40 cm of Hg. A mixture of 90% A and 10% CH_4 was used in the narrow-window detector to increase sensitivity at energies greater than 3 keV. The detector with a wide window was filled with a 90% Ne 10% CH_4 mixture which allows the energy spectrum of incident x-rays to be more readily determined. A separate gas flow system was used for each detector and consisted of a supply bottle at 2000 psig,

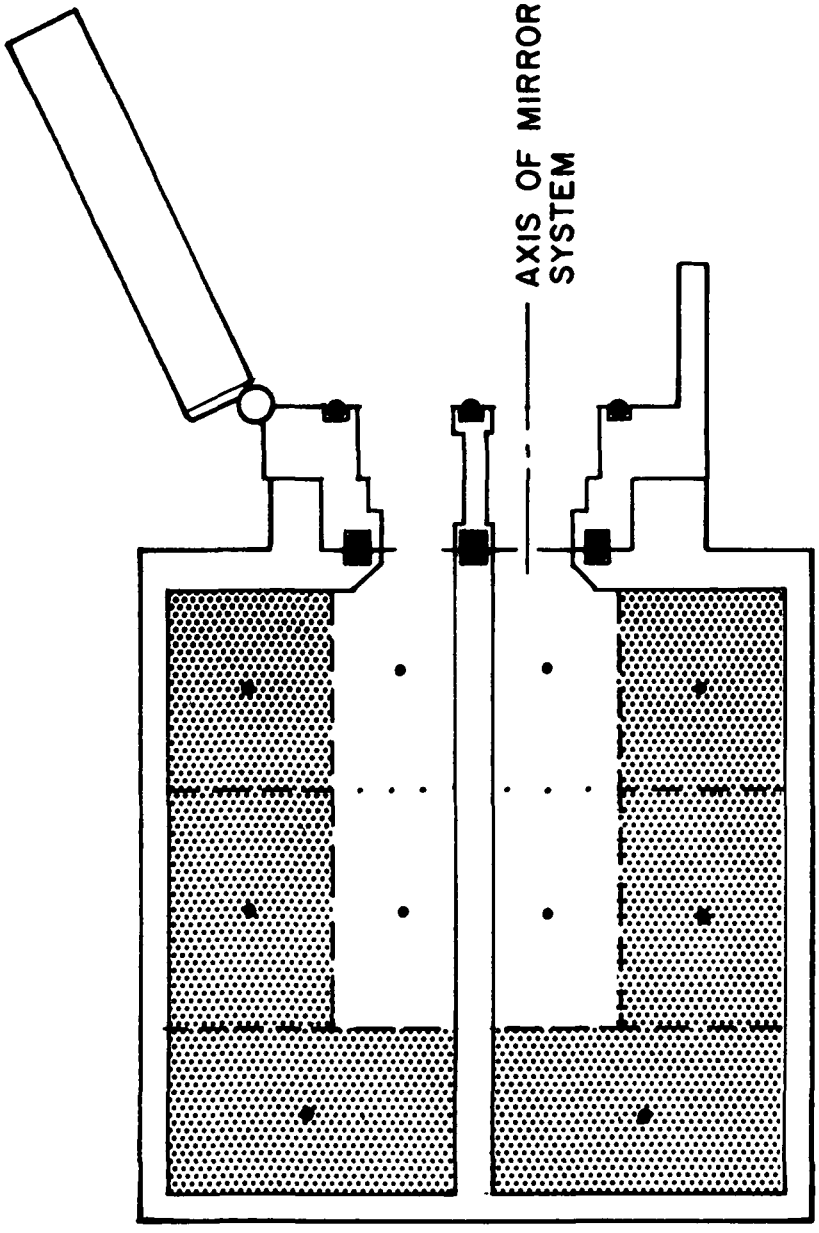

Figure 11 Cross sectional view of the Aerobee 17.08 gas flow proportional counters. The primary detectors are indicated by the central unshaded areas while the anticoincidence counters are shown as stippled regions. The hinged antichamber lid is shown in the open position which allows x-rays to be focussed on the counter windows, indicated by the apertures at the upper end of the primary detectors.

high and low pressure regulators which reduced the input pressure successively to 55 psig and 40 cm of Hg, a flow restrictor and a vacuum outlet into which the counter gas was exhausted. The vacuum outlet was maintained before launch by a forepump, during launch by an evacuated reservoir, and thereafter by the hard vacuum of space. Squib-actuated valves sealed off the vacuum reservoir at launch and vented the system to space early in the rocket flight. The pressure in each detector was measured during flight and the result transmitted via telemetry. Radioactive calibration sources of Po^{210} supplied fluorescent x-rays of Al and Ti, at 1.5 and 4.5 keV respectively, and were attached to the antichamber lid in front of each of the detectors. Calibration data were acquired by both detectors until the antichamber lid was opened 98 sec after launch, and again when the lid closed before re-entry.

Proportional counter pulses from x-rays in the energy range from 0.5 to 4.0 keV were shaped appropriately and transmitted directly via telemetry. Pulses from x-rays in the range .15 to .5 keV were separated into three energy intervals by pulse height discriminators. The outputs of these discriminators were fed into scalers and onto telemetry. In addition to rejection by the anticoincidence gas counters, non-x-ray background events were rejected by pulse risetime discrimination. The pulse height spectrum above 0.5 keV was transmitted with and without background rejection. In addition, each rejected pulse in the 'total' spectrum was identified as being 1) from an x-ray, 2) rejected by gas anticoincidence, 3) rejected by pulse risetime discrimination, or 4) both 2) and 3). These data will allow both methods of background suppression to be evaluated by examination of the spectra of rejected events.

A sealed Be-window proportional counter filled with P-10 gas was also flown on NASA 17.08. The geometric area of this detector was approximately 220 cm^2; it was sensitive in the energy range from 2 to 20 keV and had an angular collimation of $3/4^\circ$ full width at half maximum. Pulses from this counter were stretched in time and placed directly on telemetry.

IV. PRELIMINARY RESULTS OF JUNE 1971 FLIGHT

On 24 June 1971 at 0550 UT the x-ray optical system described in this report was launched from White Sands Missile Range on an Aerobee 350 rocket, NASA Aerobee 1708. In addition to the instrumentation previously discussed, two electronic star sensors with V-shaped apertures, a photomultiplier sensitive to visible star light reflected by the x-ray optics, and a 35 mm camera, were included in the payload to determine aspect. The camera had a field of view 14° by 21° and took a photograph of the star field every 1.6 sec. During the slow scans stars down to approximately 6th magnitude are visible on the film. Stars were observed during the flight by all of the aspect sensors.

As mentioned earlier, slow scans at a rate of 0.03° sec^{-1} were made over several extragalactic objects. These included the Seyfert galaxy NGC 4151, the quasar 3C 273, and the peculiar radio galaxy M 87. In addition, a scan at 0.2° sec^{-1} was made over the galactic x-ray source Sco X-1.

Data from scans across NGC 4151 and 3C 273 have not yet been reduced but preliminary indications are that if these objects have been observed at all, their counting rates are very close to counter background rates. Both of the objects are known to emit x-rays at energies greater than about 1.5 keV although no spectral data have been published. Final analysis of the flight data, if no x-rays significantly above background are detected from these objects, will allow upper limits to be placed on the previously uninvestigated part of their spectra in the range from .25 to 2 keV.

Large counting rates were observed from Sco X-1 in all of the x-ray detectors. These data, when reduced, will allow the spectrum of this source to be investigated in the range from .25 to 20 keV.

The spectrum of Sco X-1 incident on the mirror array may be determined from data acquired by the Be-window detector, and the reflected spectrum from that obtained by the gas flow proportional counters. From these flight data it will then be possible to measure the response of the optical system to a point source of x-rays, and compare it to that obtained from laboratory measurements as shown in Figure 10. This response can be measured directly in the energy range from 2 to 4 keV where data from the Be-window and the gas flow proportional counters overlap. It may be determined at energies less than 2 keV, to the extent that it is valid to extrapolate the incident spectrum observed at higher energies.

The flight data from a 3^{o} scan in the constellation Virgo are shown in Figure 12. The scan was made in a direction approximately joining the galaxies M 87 and M 84. In this figure, the counting rate in the 0.5 to 4 keV energy range obtained by the detector with a field of view of 20 arc minutes is plotted against the time from launch. The times at which the detector field of view passed over M 87 and M 84 were determined from preliminary analysis of the aspect photographs and are indicated in the figure along with the rocket altitude at these times. Data at 0.25 keV, from the carbon transmission band of the detector's polypropylene window, are not included in this plot. An increase in the counting rate was observed when the detector field of view crossed M 87; the profile of the response expected for a point source is indicated by the crosses. The distribution observed from M 87 is not consistent with that of a point source, but appears to be extended with an angular size of approximately 30 arc minutes. M 87 was not observed by the counter with the six arc minute wide field of view. The fact that only a fraction of the 30 arc minute wide source fell within the six arc minute field of view was sufficient to make M 87 unobservable by this detector.

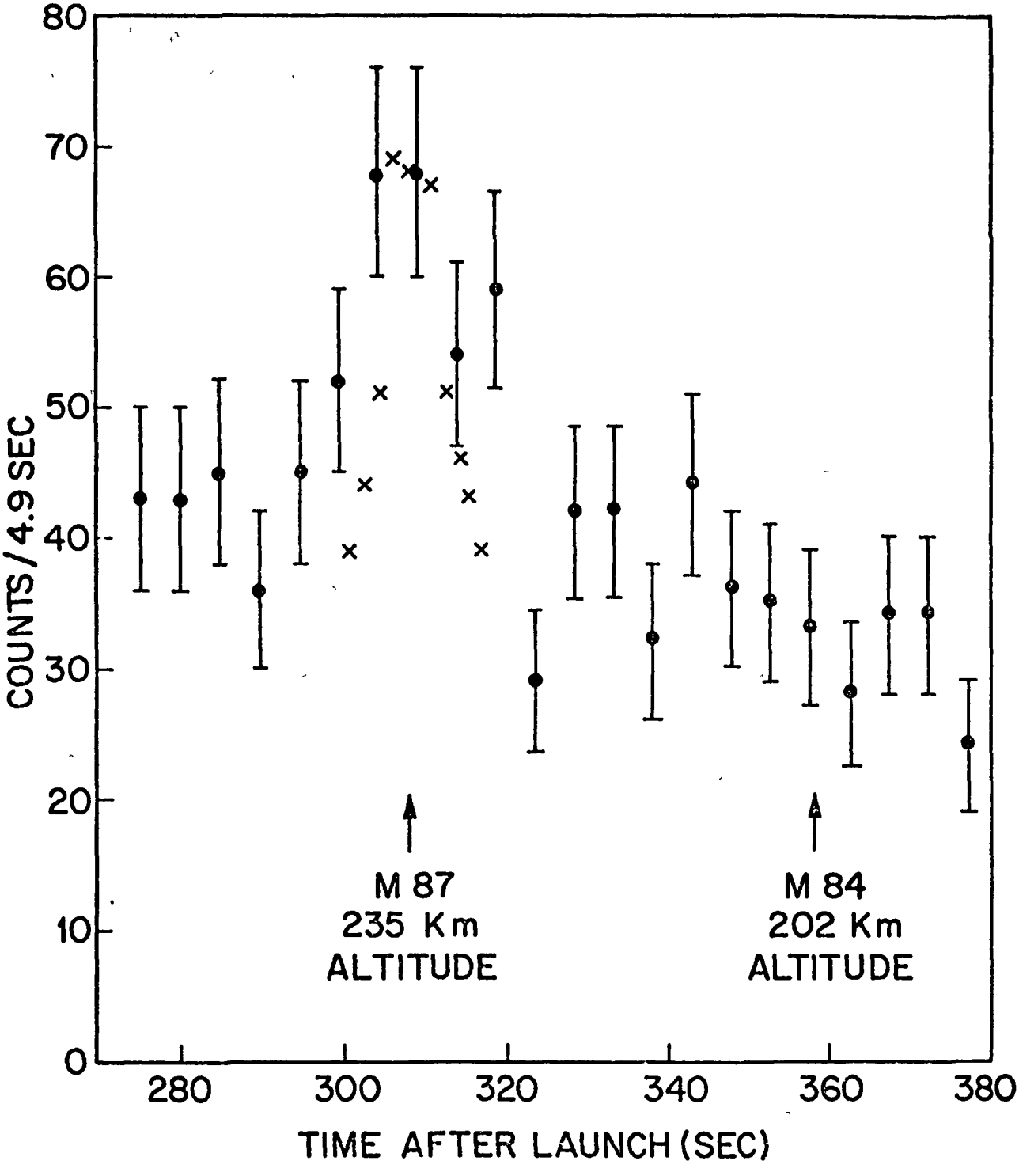

Fig. 12 Counting rate vs. time during a 3^{o} scan in the Virgo Cluster of galaxies. Data were acquired in the 0.5 to 4 keV energy range by the detector with a 20 arc minute field-of-view. The points are plotted with one sigma error bars and the crosses indicate the response of the system to a point source of x-rays. The times at which the field-of-view passed over M 87 and M 84 are shown along with the rocket altitude.

After subtracting background obtained from 23 sec of data on either side of the source, there were approximately 150 net counts from M 87 remaining in four energy bins. These data were fitted to a power law function, with an interstellar absorption, given by:

$$I = Ae^{-N_H\sigma} E^n \text{ photons } (\text{cm}^2 \text{ sec keV})^{-1},$$

where N_H is the line of sight hydrogen density in atoms cm^{-2}, σ is the attentuation coefficient for interstellar matter derived by Brown and Gould (1970), E the photon energy, A the spectral amplitude and n the index of the photon spectrum. A computer program was used which provided a least squares fit to the data and included the effects of spectral distortion by the proportional counter resolution. At the rocket altitude during this scan, attenuation of x-rays by the residual atmosphere was negligible. Results of this calculation are shown in Figure 13, where the number of counts observed in each energy interval is plotted with a one-sigma error bar. The histogram shows the number of counts in each of these intervals that are produced when a spectrum described by the following parameters is folded through the instrumental efficiencies.

$$A = 0.18 \pm 0.02, \quad N_H = 10 \pm 5 \times 10^{20}, \quad n = -3.4 \pm 0.7$$

The computer program has adjusted these three parameters so that the sum of squares of the deviation between the histogram and the observed counts is a minimum. While the data point at .25 keV is of low statistical significance, it indicates a significant lack of low energy photons in the spectrum, since the observed value falls below an extrapolation of the unattenuated power law by a factor of 50.

The best fit spectral index of -3.4 is similar to values obtained by Byram et al. (1971) and Lampton et al. (1971) from rocket flights in 1969. The amount of interstellar matter required to best fit the data yields a neutral hydrogen density approximately four times greater that that between here and the Virgo Cluster determined by 21 cm

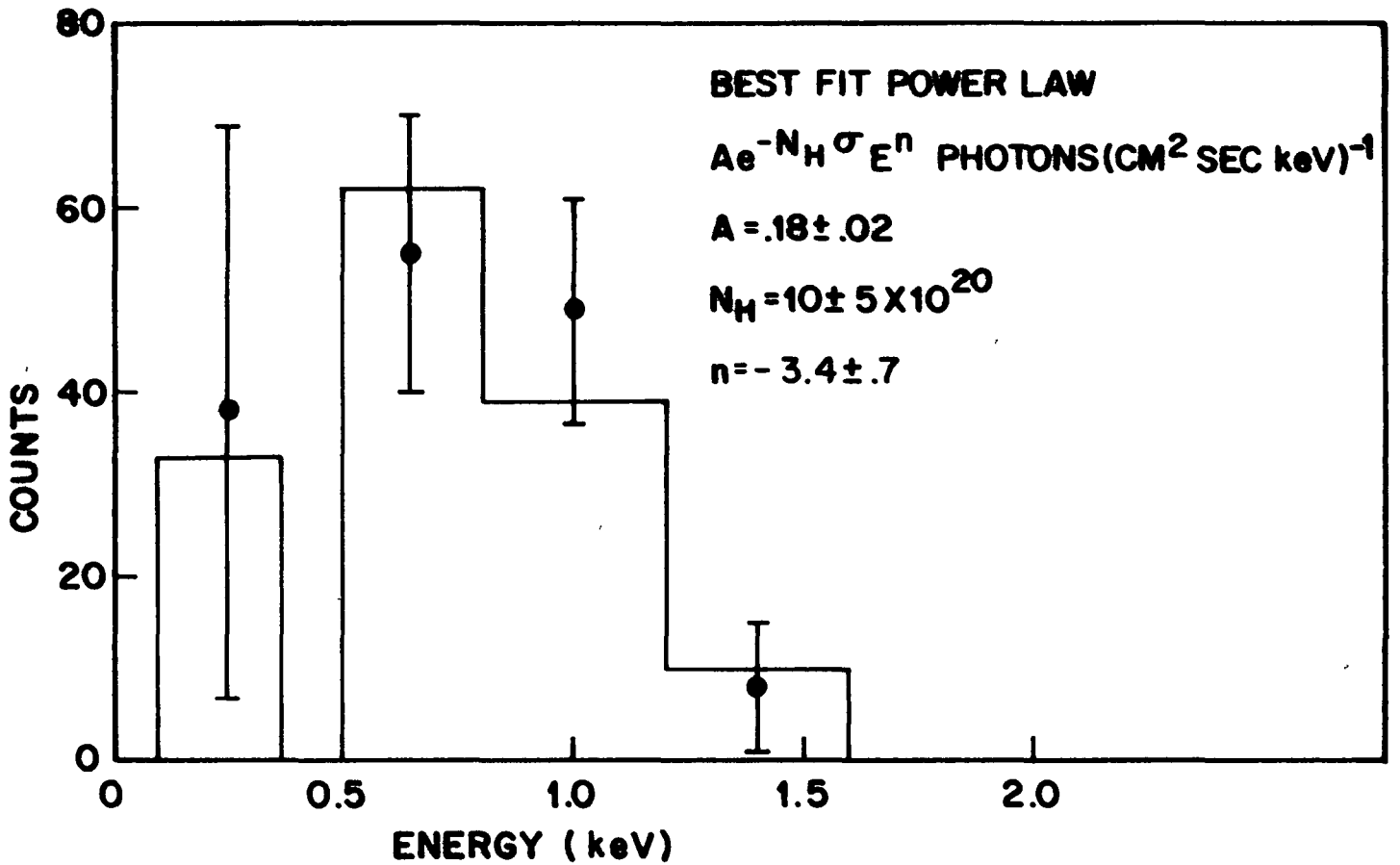

Figure 13 The number of counts observed in each energy interval from M 87 are shown by the points. One-sigma error bars have been attached to these points. The histogram shows the number of counts produced in each energy interval when the spectrum specified in the upper right corner of the figure is folded through the instruments efficiency.

emission measurements. The power in this spectrum, obtained by integrating this "best fit" function from 1 to 10 kev, is 2×10^{-10} ergs cm^{-2} $sec.^{-1}$ This is comparable to the results of Byram et al. (1971), but is substantially less than the values obtained by Lampton et al. (1971), Janes et al. (1971), Byram et al. (1966), and Friedman et al. (1967), which lie in the range from approximately 7 to 20 $\times 10^{-10}$ ergs $cm^{-2} sec^{-1}$. Part of the reason the power determined by this observation is smaller than most other measurements is because it refers to only a portion of the object which other observers have measured. Note the decrease in counting rate shown in Figure 12 near the end of the scan. This decrease may be significant as it differs by nearly three standard deviations from the rate near the source. Although it has not yet been fully analyzed, the background rates observed just before this scan, near 3C 273, are also lower than those adjacent to the position of M 87. This result is similar to that of Byram et al. (1971) in which they found a general increase in the background counting rate when their field of view was in the Virgo Cluster, but not on M 87. The power from 1 to 10 kev of 2×10^{-10} ergs $cm^{-2} sec^{-1}$ refers only to the central source. With a downward adjustment of the background rate the power from the source may approximately double in value. This would compare favorably with a value of 5×10^{-10} ergs $cm^{-2} sec^{-1}$ obtained from UHURU data by Kellogg et al. (1971).

V. CONCLUSIONS AND RECOMMENDATIONS

A. A soft x-ray detection system based on a nested array of confocal parabolic mirrors that provides a line-shaped image of a distant on-axis x-ray source has been constructed and found to be precise enough to provide minute-of-arc angular resolution during a rocket flight.

B. For the sake of economy, mirrors of future arrays should be fabricated from a material like fused silica or pyrex rather than nickel-coated beryllium. It is anticipated that the metal coating

of vitreous mirrors required to obtain more efficient reflection of x-rays at energies larger than 0.5 keV will lead to a significant amount of non-specular reflection.

C. An efficient survey of faint sources of 0.1-3 keV x-rays could be made with a pair of detection systems with intersecting line-shaped fields of view. If the interest in the survey was restricted to the less energetic x-rays, a mirror system consisting of crossed parabolic arrays might also be used. The two procedures provide comparable performance at about 1 keV.

D. Preliminary analysis of data from the June 1971 rocket flight under this contract confirms the extended nature of the x-ray source in Virgo and suggests that its structure may be complex. In particular, these data suggest the presence of a core of x-ray emission approximately 0.5° in diameter surrounded by an emitting region which is at least 2° across. This core is centered on the radio galaxy M 87. The spectrum of the Virgo source is observed to have very few low energy photons. If the observed spectral data are fitted to a power law function with an absorption factor, approximately four times more interstellar matter is required to produce the low energy x-ray attentuation than is inferred from measurements of 21 cm hydrogen emission.

VI. ABSTRACTS OF PAPERS PRESENTED AT MEETINGS

Due to the large effort devoted to construction of flight apparatus, the lack of results from the first rocket flight, and the fact that analysis of data from the June 1971 flight has just begun, publications under this contract have been severely limited. Abstracts of several talks describing the effort are given on the following pages.

Published in Bull. Amer. Astron. Soc. 1, 343, 1969.

Author please enter → CATEGORY NO. 9 (or 1)

AMERICAN ASTRONOMICAL SOCIETY

ABSTRACT OF PAPER

Abstracts should be submitted as far as possible in advance of the announced deadline of the meeting to G. C. McVittie, Secretary, American Astronomical Society, University of Illinois Observatory, Urbana, Illinois 61801. Please submit clean double-spaced copy, suitable for the printer, with a carbon on plain white paper. A copy will be furnished by the Secretary to the Bulletin of the American Astronomical Society for publication, and as voted by the Council will carry a $30 publication charge to be billed to your institution. Revisions for the Bulletin copy will be accepted by the editors until 5 days after the close of the meeting. *These revisions must be sent direct to the editors of the Bulletin, and not to the Secretary.* **BECAUSE NO GALLEY PROOFS ARE PROVIDED, THIS IS THE LAST OPPORTUNITY FOR REVISIONS.**

Title of Paper: X RAY SURVEY EXPERIMENT

Authors and Addresses for by-line:

Philip C. Fisher

Lockheed Palo Alto Research Laboratory

Palo Alto, California 94304

In view of the unanticipated strength of the cosmic x-ray emissions so far discovered, and the confusion over much of the relevant physics, a rapid sky survey of the highest practicable sensitivity to search for further surprises (especially from extragalactic objects) would seem a worthwhile enterprise. One means of conducting a survey could involve use of a grazing-incidence optical system that can simultaneously discover, locate in one coordinate per observation, and provide spectral information about x-ray sources. The apparatus could employ a gas proportional counter to detect x rays reflected by a nested array of parabolic mirrors. The mirror array itself might also be one element of a spectrograph (Fisher, P. C., and Kirkpatrick, P., Astron. J. 71, 854, 1966). While the survey system would be most useful for x rays less energetic than a few keV (that cannot be conveniently detected with large-area gas counters), sufficient sensitivity exists above this energy that all but the faintest energetic sources accessible to very-large-area counters can be observed. The dominant constraints in detecting faint extragalactic objects may well be the shortage of the less energetic x rays which results from absorption near the source, and the lack of observing time. In addition to these constraints, absorption and scattering in the interstellar medium will limit the faintest galactic sources that can be detected.

The current survey instrument is nearly two meters long and should have an effective aperture of about 80 cm^2 for x rays less energetic than a few keV. Some of the basis for, and features of, five generations of development of this experiment over the last nine years will be discussed.

This work was performed in part under National Aeronautics and Space Administration Contracts NAS 5-1174, NASw-909 and 1388, and in part under the Lockheed Independent Research Program.

I.A.U. Symposium No. 41 on New Techniques in Space Astronomy, Munich.

ROCKET PROTOTYPE OF AN X-RAY OPTICAL SYSTEM FOR SURVEYING AND LOCATING COSMIC X-RAY SOURCES

P C FISHER, L W ACTON, R C CATURA, P. KIRKPATRICK, A J MEYEROTT, and D T ROETHIG

Lockheed Palo Alto Research Laboratory, Palo Alto, Calif., U S A

The characteristics of an X-ray detection system based on an array of parabolic reflectors that provide a line-shaped focus will be described The most recent rocket instrument has an overall length of about two meters and utilizes a pair of thin-window gas-flow proportional counters for detecting the X-rays The variation of effective aperture with X-ray energy, the amount of scattering from the mirror surfaces, and the quality of the optical focus will be discussed Estimates of the sensitivity of a larger set of X-ray optics used as a survey system, and when combined with a special grating to form a spectrograph, will be presented.

This program has been carried out under the support of the National Aeronautics and Space Administration (Contracts NASw-909, 917, and 1388) and the Lockheed Independent Research Program.

DISCUSSION

E A. Trendelenburg Is it intended to fly your experiment on a satellite?

P C Fisher An experiment involving a pair of mirror arrays, and including a spectroscopic capability has been proposed for satellite use

Labuhn and Lüst (eds.), New Techniques in Space Astronomy, 182

Abstract Submitted

for the Puerto Rico Meeting of the

American Physical Society
Division of Cosmic Physics

December 1-4, 1971

Physical Review
Analytic Subject Index
Number 61.2

Bulletin Subject Heading
in which Paper should be placed
Discrete X-Ray Sources

Spectrum of Soft X-Rays from the Virgo Cluster.
R.C. CATURA, P.C. FISHER, H.M. JOHNSON and A.J.MEYEROTT, Lockheed Palo Alto Research Laboratory. -- A recent rocket experiment utilizing singly reflecting x-ray optics has extended measurements of the spectrum of x-rays from the Virgo Cluster down to 1/4 Kev. A portion of the Cluster was scanned approximately along a line passing through the galaxies M 87 and M 84. During this scan a source of x-rays was detected which had an angular extent of approximately 0.5^{o}. Precise location of the center of this source has not yet been determined, but its extent contains M 87. X-rays were detected in the range from 1/4 to 2 Kev and the spectrum shows a clear turnover at low energies. Analysis of the spectrum will be presented. This research was supported by contract NASw-1388 and the Lockheed Independent Research Program.

Submitted by

Richard C. Catura

Richard C. Catura

Orgn. 52-14, Bldg. 202

3251 Hanover Street, Palo Alto, California

REFERENCES

Brown, R. L. and Gould, R. J., 1970, Phys. Rev. D 1, 2252.

Byram, E. T., Chubb, T.A., and Friedman, H., 1966, Science 152, 66.

Byram, E. T., Chubb, T. A., and Friedman, H., 1971, Nature 229, 544.

Ershov, O. A., Brytov, I. A., and Lukirskii, A. P., 1967, Optics and Spectroscopy 22, 66.

Fisher, P. C. and Meyerott, A. J., 1966, Proc. IEEE NS-13, 580.

Janes, A. F., Pounds, K. A., and Ricketts, M. J., 1971, Nature 230, 188.

Friedman, H., and Byram, E. T., 1967, Science 158, 257.

Kellogg, E., Tannanbaum, H., Gursky, H., Giacconi, R. and Pounds, K., 1971, Paper presented at the Joint APS-AAS Divisional Meeting, San Juan, Puerto Rico.

Lampton, M., Bowyer, Stuart, Mack, J. E. and Margon, B., 1971, Ap. J. Letters 168, L1.

Rieser, L. M. Jr., 1957, Reflection of X-Rays and the Reflection Microscope, X-Ray Microscopy and Microradiography, Edited by Casslett, V. E., Engstrom, Arne, and Pattee, H. H., Academic Press, Inc., New York.

Veigele, William J., Briggs, E., Bracewell, B., and Donaldson, M., 1969, Kaman Nuclear, KN-798-69-2.

Wuerker, Ralph Fredrick, 1960, Spectral Reflectance by Solids of Carbon K Radiation, Stanford University Dissertation.

APPENDIX A

Many computer programs were developed at this laboratory over several years to aid in the design of nested and baffled arrays of mirrors and to predict their effective aperture. This work lead to the Fortran V program given in this appendix. The program calculates the basic design parameters as well as the effective aperture for an on-axis source of the set of nested nickel-coated parabolic mirrors used on the flight of Aerobee 17.08. A Cartesian coordinate system, whose origin is at the center of the entrance aperture of the on-axis detector, is used in this program.

Input parameters needed to run the code include:

a) MAXN, the number of mirrors nested together on one side of the system,
b) KL and L, the x values of the ends of the outside mirror (KL<L),
c) H(1), the y value at L for the outside mirror,
d) Y_U and Y_D, the y values of the detector aperture,
e) ANGIN, the angle of incidence (deg) of the incident ray with respect to the x-axis. Its sense is positive when the angle of incidence to the mirror is increased, and
f) T(I), the respective thicknesses of the mirrors.

One side of the mirror array is calculated as one data set.

This code will stack the set of MAXN mirrors so that there is no obstruction from one mirror to another for radiation reflected into the desired detector aperture. The parameters of this stacking include the Q values in the equation $y = \sqrt{Qx + Q^2/4}$ (an equation for a parabola with its focus at the origin); the y values at the ends of the mirror,

G and H; and the positions and allowable thicknesses for the inner and outer baffles.

An integration is performed over elemental portions of each mirror to obtain the effective beam breadths as a function of energy. These integrations were performed using the reflection efficiency information discussed in Section III D. The code yields the reflectivity for each portion of each mirror as a function of x coordinate and angle of incidence, and in addition lists the integrated results for the complete mirror. A study of these data gives an understanding of how the individual mirrors contribute to the aperture of the array. It should be noted that the resultant effective beam breadth integrations are valid only for an on-axis source. The effective beam breadth calculated for off-axis sources might include contributions from radiation which did not actually reach the detector window. To use this code for such sources one must include a constraint that the radiation was not intercepted by a baffle and does fall within the detector window. A computer listing of the program follows:

```
@FOR,IS PARSET
      DIMENSION  H(99), G(99), T(99), XT(99), YT(99), XS(99), YS(99),
     X     TI(2), DA(2), M(99), Q(99), HG(20), SUMEBB(15), SUBTOT(15)
      DIMENSION   UMAX(99)
      DIMENSION     CHRDNG(15)
      DIMENSION     DYS(99)
        DIMENSION   AT(99), AS(99)
      REAL   KL, K, L, KEV
      REAL     MAXANG(15), MINANG(15)
      COMMON   /BLK/   EFBB(20,15), NMIR, KEV(15), XLAM(15), ANGIN
      COMMON     /OUTPUT/     IIO
      COMMON   /BLK3/   G, XS, YS, Q, YD, KL
      RPD = 0.0174532925
    1 READ(5,10)   MAXN, KL, L, H(1), YD, YU, ANGIN, (T(I),I=1,MAXN)
   10 FORMAT(I2, / 6F10.4, /(8F10.4))
      IF(MAXN.GT.20)     CALL MERR
C     IF INTERMEDIATE DATA IS WANTED, IIO SHOULD BE 1, OTHERWISE 0.
      READ(5,11)   IIO
   11 FORMAT(I1)
      DO 15   I = 1, MAXN
      IF(T(I).LT.0.00001)   T(I) = T(I-1)
   15 CONTINUE
      CALL TOD(8,TI)
      CALL DATE(9,DA)
C
C
C     ***************************************************************************
C
C
      K = KL/L
      Q(1) = 2.0 * (SQRT(L**2 + H(1)**2) - L)
      G(1) = SQRT(Q(1) * KL + Q(1)**2 / 4.0)
      N = 1
      CALL BAFFLE(Q(N),KL,L,G(N),H(N),YU,YD,XT(N),YT(N),AT(N),XS(N),YS(N
     X     ), AS(N),N)
      M(1) = 1
      NMIR = 1
      CALL REFLCT(Q(1), KL, L)
      HG(1) = H(1) - G(1)
      DO 100   N = 2, MAXN
      M(N) = N
      G(N) = K * H(N-1) + (1.0-K)*YD - T(N)
      Q(N) = 2.0 * (SQRT(KL**2 + G(N)**2) - KL)
      H(N) = SQRT(Q(N) * L + Q(N)**2 / 4.0)
      HG(N) = H(N) - G(N)
      CALL BAFFLE(Q(N),KL,L,G(N),H(N),YU,YD,XT(N),YT(N),AT(N),XS(N),YS(N
     X     ), AS(N),N)
      NMIR = N
      CALL REFLCT(Q(N), KL, L)
  100 CONTINUE
      DO 101   N = 2, MAXN
  101 CALL GETDYS(DYS(N), N)
C
C
C     ***************************************************************************
C
C
      WRITE(6,200)   DA, TI, KL, L, K, YD, YU, ANGIN
  200 FORMAT(1H1 'PARABOLIC MIRRORS WITH FOCUS AT ORIGIN'  /
     X     1X 'WRITTEN FOR P C FISHER BY D T ROETHIG ON 01-31-69' /
     X     1X 'EXECUTED ON ' A6, A3, ' AT ' A6, A2, /
```

```
     X      ' MIRRORS ARE COATED WITH NICKEL.' ///////
     X      1X 'KL = ' F5.1, /
     X      1X 'L  = ' F5.1, /
     X      1X 'K  = ' F7.5, /
     X      1X 'YD = ' F6.3, /
     X      1X 'YU = ' F6.3, /
     X      1X 'INCREASE IN ANGLE OF INCIDENCE = ' F6.3)
       WRITE(6,250)   (M(I), Q(I), G(I), H(I), XT(I), YT(I), AT(I),
     X      XS(I), YS(I), DYS(I), AS(I), T(I), I = 1, MAXN)
  250 FORMAT(1HO // 2X 'M' 10X 'Q' 14X 'G' 15X 'H' 9X 'XTU' 8X
     X      'YTU' 8X 'AT' 7X 'XSU' 8Y 'YSU' 6X 'AYS' 8X 'AS' 8X 'MT' ///
     X      (I3, 1P3E16.6, 0P8F10.5)   //)
C     ***************************************************************
      DO 275   I = 1, MAXN
      SLOPE = (H(I) - G(I))/(L - KL)
      THETA = ATAN(SLOPE)
      B = G(I) - KL*(H(I)-G(I))/(L-KL)
      XMAX = Q(I)/4.0 * (1.0/(SLOPE**2) - 1.0)
  275 JMAX(I) = COS(THETA)*(SQRT(Q(I)*XMAX+Q(I)**2/4.0)-SLOPE*XMAX-B)
      WRITE(6,280)   (JMAX(I), I = 1, MAXN)
  280 FORMAT(1HO //' MAXIMUM DEPTHS OF MIRRORS IN INCHES --->'
     X      E10.5, 3E15.5, /(36X 4E15.5))
C     ***************************************************************
C     ***************************************************************
      DO 300   J = 1, 15
      DO 300   I = 1, N
      SUBTOT(J) = SUBTOT(J) + EFBB(I,J)
  300 SUMEBB(J) = SUMEBB(J) + EFBB(I,J)
      WRITE(6,350)   KEV, XLAM, ((I,(EFBB(I,J),J=1,15),HG(I),I=1,NMIR))
  350 FORMAT(2H1 15F8.3,/2X15F8.3, 5X 'H-G' ///
     X      (1X I2, 1X 16(1PE8.2)/))
      WRITE(6,400)   SUBTOT, SUMEBB
  400 FORMAT(   /   3X  15(1PE8.2), / 3X 15(1PE8.2))
C     ***************************************************************
      CALL MOVER(0, 0, SUBTOT, 1, 15)
      IF(ABS(ANGIN).LT.0.0001)     GO TO 1
      DO 460   I = 1, MAXN
      IF(I.EQ.MAXN)     GO TO 450
      MAXANG(I) = ATAN((G(I)-H(I+1)-T(I+1)),(L-KL))/RPD
  450 MINANG(I) = -ATAN(SQRT(1.0/(4.0*L/Q(I) + 1.0)))/RPD
      CHRDNG(I) =-ATAN((H(I)-G(I))/(L-KL))/RPD
  460 CONTINUE
      WRITE(6,500)     (I, MAXANG(I), MINANG(I), CHRDNG(I), I = 1, MAXN)
  500 FORMAT(1HO///' THE FOLLOWING GIVES THE MAXIMUM, MINIMUM AND CHORD'
     X      ' ANGLES:'   ///   (I10, 3F10.5))
      GO TO 1
      END
*FOR,IS BAFFL
      SUBROUTINE BAFFL(KL, L, G, H, YU, YD, XT, YT, XS, YS, N)
      REAL   KL, L, K
      K = KL/L
      XT = L * (G - 2.0 * YD) / (H - ((1.0+K)/K) * YD)
      YT = G + (XT/KL - 1.0) * YD
      IF(N.EQ.25)   YT = YT - 0.005
      XS = (H - 2.0*YU) / ((YT-YU)/XT - YU/L)
      YS = H - YU + (H-2.0*YL)/(L*(YT - YU) / (XT*YU) - 1.0)
      RETURN
      END
*FOR,IS INTPLT
      SUBROUTINE INTPLT(R, L, B, J, S)
C     THIS SUBROUTINE IS FOR NICKEL .
```

```
C     B IS THE ANGLE IN DEGREES.
C     R IS I/I0.
C     THE R'S ARE GIVEN FOR ANGLES 0, 1, 2, 3, 4, 5, AND 6 DEGREES.
C     L IS WAVELENGHT IN ANGSTROMS,
      COMMON   /OUTPUT/   IIO
      REAL   L
      DIMENSION   R16(7), R20(7), R40(7)
      DATA   R16 / 0.91, 0.72, 0.28, 0.05, 0.0, 0.0, 0.0/
      DATA  R20/ 0.95, 0.92, 0.82, 0.65, 0.30, 0.05, 0.00/
      DATA   R40 / 0.95, 0.91, 0.82, 0.72, 0.64, 0.53, 0.42/
      RPD = 0.01745329252
      B = B / RPD
      IF(B.GE.6.0 .OR. B.LT.0)     GO TO 50
      I = B
      IF(J-14)     16, 20, 40
   16 R = R16(I+1) - (B-I)*(R16(I+1) - R16(I+2))
      GO TO 50
   20 R = R20(I+1) - (B-I)*(R20(I+1) - R20(I+2))
      GO TO 50
   40 R = R40(I+1) - (B-I)*(R40(I+1) - R40(I+2))
   50 IF(IIO.EQ.0)     GO TO 70
      WRITE(6,60)   B, R, S
   60 FORMAT(15X 3E15.7)
   70 B = B * RPD
      RETURN
      END
@FOR,IS RATIO
      SUBROUTINE RATIO(RATIO, THETA, D, M, Y, S)
C     D EQUALS ONE MINUS THE INDEX OF REFRACTION.
C     M EQUALS THE LINEAR ABSORPTION COEFFICIENT.
C     Y EQUALS RIESER'S BETA/DELTA.
C     X EQUALS THE INCIDENT ANGLE / SQRT(2*DELTA)
      COMMON     /OUTPUT/     IIO
      REAL   M
      IF(THETA.LT.0.0)     RETURN
      RPD = 0.01745329252
      X = THETA / SQRT(2.0 * D)
      A = SQRT(2.0) * X
      B = SQRT(SQRT((X*X-1.0)**2+Y*Y)+X*X-1.0)
      C = SQRT((X*X-1.0)**2+Y*Y)-X*X+1.0
      RI = ((A-B)**2+C)/((A+B)**2+C)
      THETA = THETA / RPD
      IF(IIO.EQ.0)     GO TO 20
      WRITE(6,10)   X, THETA, RI, S
   10 FORMAT(4E15.7)
   20 THETA = THETA * RPD
      RATIO = RI
      RETURN
      END
@FOR,IS REFLCT
      SUBROUTINE REFLCT(D, KL, Z)
C     CALCULATION OF MIRROR REFLECTIVITIES
C     THIS INCLUDES A DETERMINATION OF EFFECTIVE BEAM BREADTH,
C     WRITTEN ON 03-18-69,
      DIMENSION   L(15),          B(101), O(9), TI(2), DA(2), A(15),
     X     R(101), S(31)
      REAL   L, M, KEV, KL
      COMMON   /BLK/   EFBB(20,15), NMIR, KEV(15), XLAM(15), ANGIN
      COMMON     /OUTPUT/     IIO
      DATA O/30HNICKEL REFLECTIVITY              , 4*6H        /
      YP(X) = SQRT(Q/4.0) / SQRT(X+Q/4.0)
```

```
      DATA  L /2,0, 2.75, 3.0, 3.5, 4.0, 4.5, 5.0, 6.0, 7.0, 8.339,
     X     10.0, 11.0, 16.0, 20.0, 40.0/
      RPD = 0.01745329252
      PI = 3.14159265
      CONST = 4.0 * PI
      CALL TOD(8,TI)
      CALL DATE(9,DA)
      DX = (Z-KL)/30.0
      DO 100   I = 1, 15
      KEV(I) = 12.39644 / L(I)
      XLAM(I) = L(I)
      IF(I.EQ.2. OR .I.EQ.10)   GO TO 110
      IF(I.GE.13)   GO TO 110
      M = 10.0**(2.15+2.66*ALOG10(L(I)))
      D = 6.25E-05*(L(I)-1.3) + 0.305E-05*(L(I)-1.3)**2
      Y = (M*L(I)/(CONST*D))*1.0E-06
    2 IF(IIO.EQ.0.)     GO TO 6
      WRITE(6,3)   DA, TI, 0, L(I), KEV(I), NMIR, M, D, Y
    3 FORMAT(1H1 51HRIESER TYPE CALCULATION OF SOFT X-RAY REFLECTIVITY /
     X   1X      52HWRITTEN FOR PAUL KIRKPATRICK BY DT ROETHIG: 11-25-68
     X / 1X     12HEXECUTED ON  A6, A3, 4H AT A6, A2, / 1X 9A6, /
     X   1X      25HWAVELENGTH IN ANGSTROMS = 1PE9.3,  /
     X   1X      25H(OR) ENERGY IN KEV      = 1PE9.3, /
     X   1X      25HMIRROR NUMBER           = I2, /
     X   1X      25HLINEAR ABSORP. COEFF.   = E9.3,  /
     X   1X      25H1.0 - REFRACTIVE INDEX  = E9.3,  /
     X   1X      25HRIESER'S Y VALUE        = E9.3,      /  /
     X   5X 10HRIESER'S X  4X 11HTHETA (DEG) 8X 4HI/IO 7X
     X     11HX COORDNATE   /)
    8 DO 10   J = 1, 31
      X = KL + FLOAT(J-1) * DX
      S(J) = X
      B(J) = ATAN(YP(X))  + ANGIN * RPD
      IF(I.EQ.2. OR .I.EQ.10)   GO TO 11
      IF(I.GE.13)   GO TO 9
      CALL RATIO(R(J), B(J), D, M, Y, S(J))
      GO TO 10
   11 CALL INTMEY(R(J), L(I), B(J), I, S(J))
      GO TO 10
    9 CALL INTPLT(R(J), L(I), B(J), I, S(J))
   10 R(J) = R(J) * (YP(S(J))+TAN(ANGIN*RPD))*COS(ANGIN*RPD)
      CALL SMPSON(S, R, 031, A(I))
      EFBB(NMIR,I) = A(I)
      IF(IIO.EQ.0.)     GO TO 100
      WRITE(6,30)   A(I)
   30 FORMAT(1H0 3X 'EFFECTIVE BEAM BREADTH = ' E16.7)
  100 CONTINUE
      RETURN
  110 M = 0.0
      D = 0.0
      Y = 0.0
      IF(IIO.EQ.0.)     GO TO 8
      WRITE(6,120)   DA, TI, 0, L(I), KEV(I), NMIR
  120 FORMAT(1H1 51HRIESER TYPE CALCULATION OF SOFT X-RAY REFLECTIVITY /
     X   1X      52HWRITTEN FOR PAUL KIRKPATRICK BY DT ROETHIG: 11-25-68
     X / 1X      12HEXECUTED ON  A6, A3, 4H AT A6, A2, /  1X 9A6, /
     X   1X      25HWAVELENGTH IN ANGSTROMS = 1PE9.3,  /
     X   1X      25H(OR) ENERGY IN KEV      = 1PE9.3, /
     X   1X      25HMIRROR NUMBER           = I2, ///
     X   5X 10H             4X 11HTHETA (DEG) 8X 4HI/IO 7X
     X     11HX COORDNATE   /)
```

```
      GO TO 8
      END
@FOR,IS SMPSON
      SUBROUTINE SMPSON(X, Y, N, AREA)
C     THE Y VALUES MUST BE EQUALLY SPACED IN X,
C     THERE MUST BE AN ODD NUMBER OF Y'S, IE, N MUST BE ODD.
      DIMENSION   X(1001), Y(1001)
      AREA = 0.0
      IF(N.LT.5)      RETURN
      IF(N.GT.1001)      RETURN
      IF(MOD(N,2).EQ.0)      RETURN
      HO3 = ( X(2)-X(1) )/ 3.0
      L = N - 2
      M = N - 1
      DO 5   I = 2, M, 2
    5 AREA = AREA + 4.0 * Y(I)
      DO 10   I = 3, L, 2
   10 AREA = AREA + 2.0 * Y(I)
      AREA = ( AREA + Y(1) + Y(N) ) * HO3
      RETURN
      END
@FOR,IS INTMEY
      SUBROUTINE INTMEY(R, L, B, J, S)
C     THIS SUBROUTINE IS FOR NICKEL.
      DIMENSION   R275(21), R834(45)
      COMMON   /OUTPUT/   IIC
C     DATA   R275/ .735, .732, THIS SET NICKEL
C     DATA R834/,85,.845,.84,.835,.825,        THIS SET NICKEL
C     DATA R275/,872,.854,.836,.81,.78    THIS SET GOLD
C     DATA R834/,830,.825,.820,.81       THIS SET GOLD
      DATA   R275/ .735, .732, .728, .722, .710, .693, .671, .646, .617,
     X     .585, .549, .505, .450, .376, .250, .115, .055, .035, .023,
     X     .018, .014/
      DATA R834/,85,.845,.84,.835,.825,.815,.805,.79,.77,.75,.725,.705,
     X,885,.66,.64,.62,.6,.575,.555,.535,.51,.49,.47,.445,.425,.405,
     X,38,.36,.34,.315,.295,.275,.25,.225,.205,.185,.165,.14,.12,.1,
     X,08,.055,.035,.01,.00/
C     DATA R275/,872,.854,.836,.81,.78,.75,.705,.66,.61,.56..504,.448,
C    X   .392,.34,.29,.242,.2,.176,.114,.076,.048/
C     DATA R834/,830,.825,.820,.815,.807,.8,.79,.78,.77,.76,.748,.735,
C    X   .725,.71,.697,.683,.666,.652,.635,.62,.602,.582,.562,.544,.52,
C    X   .501,.48,.457,.434,.408,.384,.36,.34,.32,.3,.28,.265,.25,.235,
C    X   .22,.205,.191,.18,.167,.156/
      RPD = 0.01745329252
      B = B / RPD
      IF(B.LT.0.0)      GO TO 100
      IF(B.GT.1.0.AND.J.EQ.2)   GO TO 100
      IF(B.GT.2.2.AND.J.EQ.10)   GO TO 100
      IBLO = (B*100.0) / 5.0  +  1.0001
      IBHI = IBLO + 1
      IF(J.EQ.2)
     XR = R275(IBLO) - (R275(IBLO)-R275(IBHI))*(B-FLOAT(IBLO-1)*.05)/.05
      IF(J.EQ.10)
     XR = R834(IBLO) - (R834(IBLO)-R834(IBHI))*(B-FLOAT(IBLO-1)*.05)/.05
      GO TO 110
  100 R = 0.0
  110 IF(IIO.EQ.0)      GO TO 300
      WRITE(6,200)   B, R, S
  200 FORMAT(15X 3E15.7)
  300 B = B * RPD
      RETURN
```

```
      END
@FOR,IS GETDYS
      SUBROUTINE GETDYS(DYS, N)
      REAL   KL
      DIMENSION   G(99), XS(99), YS(99), Q(99)
      COMMON   /BLK3/   G, XS, YS, Q, YD, KL
      B = ATAN(KL/(G(N-1)-YD))
      P = ASIN(-YD*SIN(B)/SQRT(G(N-1)**2+KL**2))
      DG = (XS(N)-KL) * TAN(P)
      DYS = G(N-1) - YS(N) - DG
      RETURN
      END
@FOR,IS BAFFLE
      SUBROUTINE BAFFLE(Q,KL,L,G,H,YU,YD,XT,YT,AT,XS,YS,AS,N)
      REAL   KL, L
      YP(X) = SQRT(Q/4.0) / SQRT(X + G/4.0)
      RPD = 0.0174532925
C
C
      B = ATAN(YP(KL))
      BPT = ATAN((G-YD)/KL)
      T = BPT - B
      A = T - B
      XT = (KL*TAN(A)+G-YD)/((H-YD)/L+TAN(A))
      YT = (H-YD)*XT/L + YD
      AT = A / RPD
C
C
C
C
      B = ATAN(YP(L))
      BPT = ATAN((H-YU)/L)
      T = BPT - B
      A = B - T
      XS = (YU+L*TAN(A)-H)/(TAN(A)+(YU-YT)/XT)
      YS = TAN(A) * (XS-L) + H
      AS = A / RPD
      END
@FIN
@@
```

APPENDIX B

A computer program was written in Hewlett Packard BASIC to calculate the theoretical effective beam breadth subtended by the off-axis detector as a function of the incident angle radiation has with respect to the system axis, θ_{SYM}. A wavelength range of 2 to 11 A in steps of 0.5 A was used. A listing of this program is included below.

The procedure of Rieser (1957) was used to calculate the reflectivities as a function of angle of incidence to each mirror (See Appendix A). Thirty-one positions were chosen along each of the 20 inch long mirrors. If, for a given angle of incidence, the radiation was not obstructed by a baffle and had the proper reflected angle to reach the off-axis detector window, the increment of beam breadth for that portion of the mirror was added to the integral yielding the effective beam breadth, EBB. The effective aperture of the mirror array is the product of EBB and the unobstructed width of the mirrors.

The machine output gives the wavelength and energy of the radiation followed by a set of θ_{SYM} angles, each with its corresponding EBB. Simpson's rule is used to integrate the EBB over the θ_{SYM} set. The sum of the EBB is also given. This output is written for each of the wavelengths from 2 to 11 A. A sample output for 1.5 keV x-rays follows the end of the listing of the computer code.

```
READY
TAPE

1  DIM T[13]
50  DIM X[31],R[31],P[8]
60  DEF FNA(X)=SQR((Q/4)/(X+Q/4))
70  LET R1=1.74533E-02
80  MAT  READ P
90  DATA .306478,.180567,9.95722E-02,4.35619E-02
100  DATA .306478,.161481,7.44358E-02,2.22874E-02
110  REM
120  FOR W=2 TO 11 STEP .5
130  LET E=12.3966/W
132  LET M=10↑(2.15+2.66*LOG(W)/LOG(10))
134  LET D=6.25000E-05*(W-1.3)+3.05000E-06*(W-1.3)↑2
136  LET Y=(M*W/(4*3.14159*D))*1.00000E-08
137  LET C4=Y*Y
138  PRINT
139  PRINT W,E
140  LET T3=-.2
150  FOR K=1 TO 13
151  LET T[K]=0
155  LET A=T3-(K-1)*5.00000E-02
160  FOR Z=1 TO 8
165  LET V=Z
170  IF Z<5 THEN 185
175  LET V=-Z+4
180  LET A=ABS(A)
185  LET Q=P[Z]
189  IF Z>4 OR A>-.516 THEN 305
190  LET A2=0
191  GOTO 535
200  REM
290  REM
300  REM
305  LET K1=0
310  FOR J=1 TO 31
320  LET X[J]=52+(J-1)*20/30
324  LET C1=FNA(X[J])
325  LET D1=ATN(C1)
330  LET B=D1+A*R1
331  LET Y2=SQR(Q*X[J]+Q*Q/4)
332  LET Y3=X[J]*TAN(2*D1+A*R1)
333  LET Y4=ABS(Y2-Y3)
334  IF Y4<.65 AND Y4>.3 THEN 340
335  LET R[J]=0
336  LET K1=K1+1
337  GOTO 390
340  LET X1=B/SQR(2*D)
342  LET C2=X1*X1-1
344  LET C3=C2↑2
350  LET A1=SQR(2)*X1
360  LET B1=SQR(SQR(C3+C4)+C2)
370  LET C=SQR(C3+C4)-C2
380  LET R[J]=((A1-B1)↑2+C)/((A1+B1)↑2+C)
```

```
384   LET C5=A*R1
385   LET R[J]=R[J]*(C1+TAN(C5))*COS(C5)
390   NEXT J
400   REM
410   REM
420   LET A2=0
425   IF K1=31 THEN 535
430   LET H=(X[2]-X[1])/3
440   FOR U=2 TO 30 STEP 2
450   LET A2=A2+4*R[U]
460   NEXT U
470   FOR U=3 TO 29 STEP 2
480   LET A2=A2+2*R[U]
490   NEXT U
500   LET A2=(A2+R[1]+R[31])*H
510   REM
520   REM
535   LET T[K]=T[K]+A2
540   NEXT Z
544   PRINT AJT[K]
550   NEXT K
560   LET A3=0
570   LET H=5.00000E-02/3
580   FOR U=2 TO 12 STEP 2
590   LET A3=A3+4*T[U]
600   NEXT U
610   FOR U=3 TO 11 STEP 2
620   LET A3=A3+2*T[U]
630   NEXT U
640   LET A3=(A3+T[1]+T[13])*H
650   LET A4=0
660   FOR U=1 TO 13
670   LET A4=A4+T[U]
680   NEXT U
690   PRINT TAB(13);A3
691   PRINT TAB(13);A4
700   NEXT W
9999   END
```

```
120 FOR W=12.3966/1.5 TO 9 STEP 10
RUN

 8.2644        1.5
 .2            0
 .25           .26171
 .3            1.09945
 .35           1.44171
 .4            1.41413
 .45           1.3819
 .5            1.34517
 .55           .486356
 .6            .289043
 .65           .141406
 .7            2.90731E-02
 .75           0
 .8            0
                .386768
                7.88996

READY
```